Thomas Prokscha :: Low-Energy Muons Group :: Paul Scherrer Institut

PSI Muons: the Swiss Muon Source (SμS)

Muon Spectroscopy Training School, March 23rd 2018, ISIS

PAUL SCHERRER INSTITUT

Outline

1. Muon facilities in the world
2. Generation of continuous/pulsed muon beams
3. Pros and Cons of continuous/pulsed muon beams in μSR
4. μSR Instrumentation at the Swiss Muon Source SμS
5. The unique low-energy μSR facility at SμS for μSR studies on a nanometer depth scale (10 – 200 nm, thin films, near-surface regions, heterostructures) and LE-μSR applications

Accelerator muons for μSR

Accelerator muons (keV-MeV): ~100% polarization, depth resolution few nm to mm, lateral resolution mm to cm
measuring magnetic field distributions/fluctuations

intensity: 1000 Muons/second/cm^2 (keV) up to 10^7 Muons/second/cm^2 (MeV)

requires a proton accelerator (E_p > 500 MeV, I_p > 100 μA)

continuous μ beams: TRIUMF, PSI

pulsed μ beams: ISIS (50 Hz), J-PARC (25 Hz)

Projects: MuSIC, Osaka (continuous)
CSNS (China, pulsed)
RAON (South Korea, continuous)
SNS (Oak Ridge, pulsed)

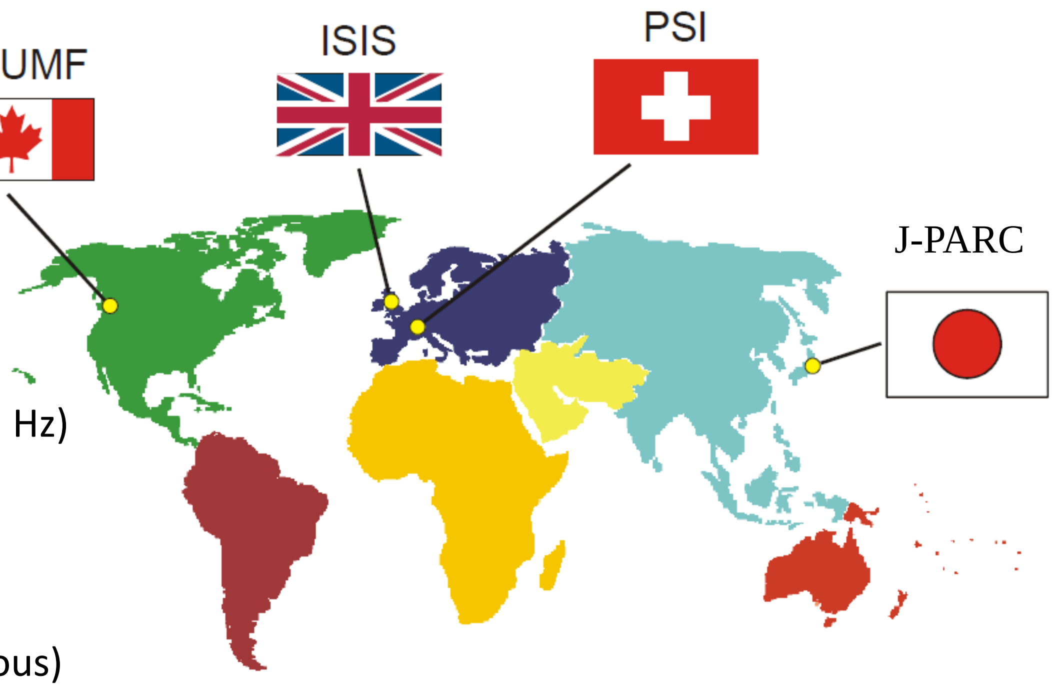

μSR facilities of the world.

http://musr.ca/intro/musr/muSRBrochure.pdf

PAUL SCHERRER INSTITUT PSI

Two muon facilities in Europe

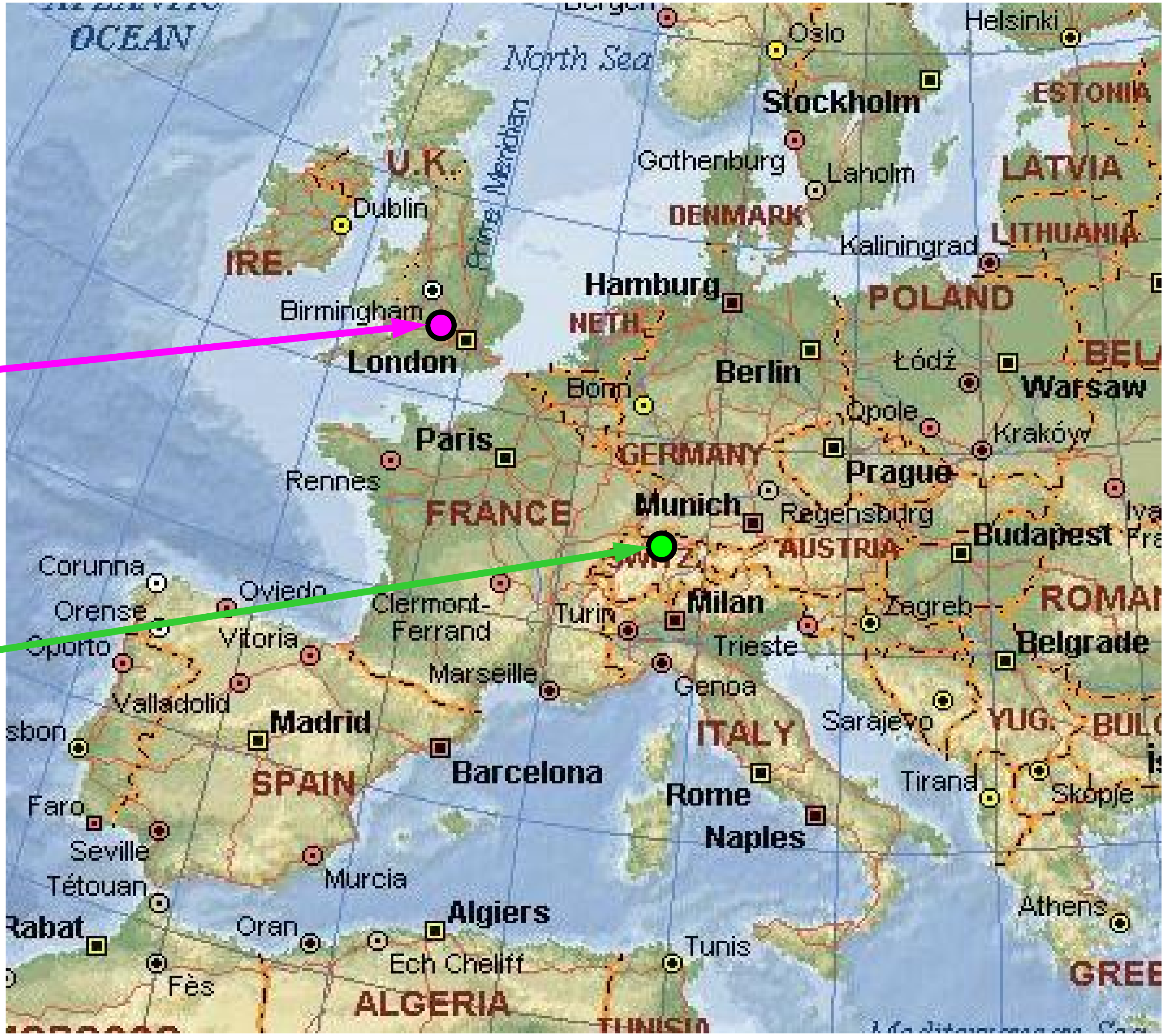

RAL/ISIS:

50 Hz pulsed muon beams

PSI:

continuous muon beams

PSI and its large scale facilities

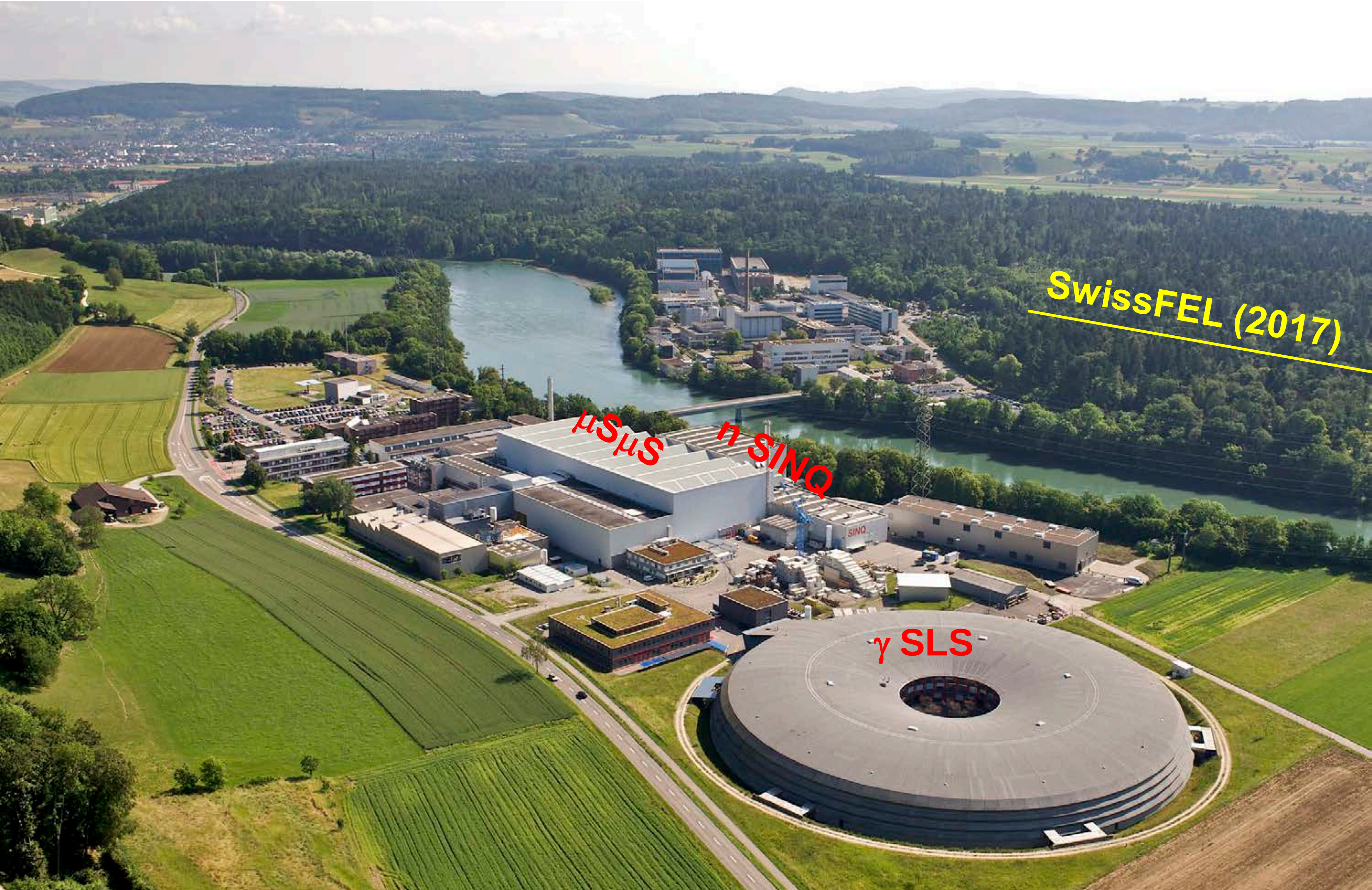

Accelerator muons

How to accelerate protons to energies > 300 MeV (pion production threshold) **and proton beam currents I_p > 100 μA** (to generate muon/pion beam with high intensities > 10^7/s) ?

Isochronous Cyclotron: compact, operated at tens of MHz RF frequency (**quasi-continuous muon beams**), constant RF frequency, constant (in time) magnetic field increasing with radius. Beam energy < 1 GeV (limited by magnetic field of magnets with saturation field of 2 T).

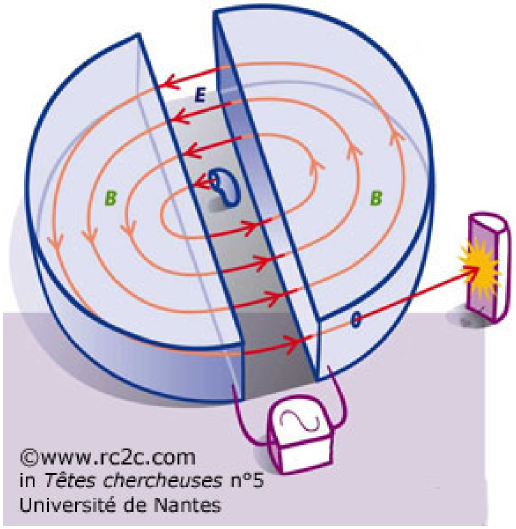

Synchrotron: can be very large (CERN LHC: 27 km) to achieve highest energies (TeV). Magnetic field synchronized with particle energy: this requires ramping of magnets which can be done at GeV energies with 50 Hz (**pulsed muon beams, with muon pulse widths of typically 100 ns**). Needs an "injection accelerator".

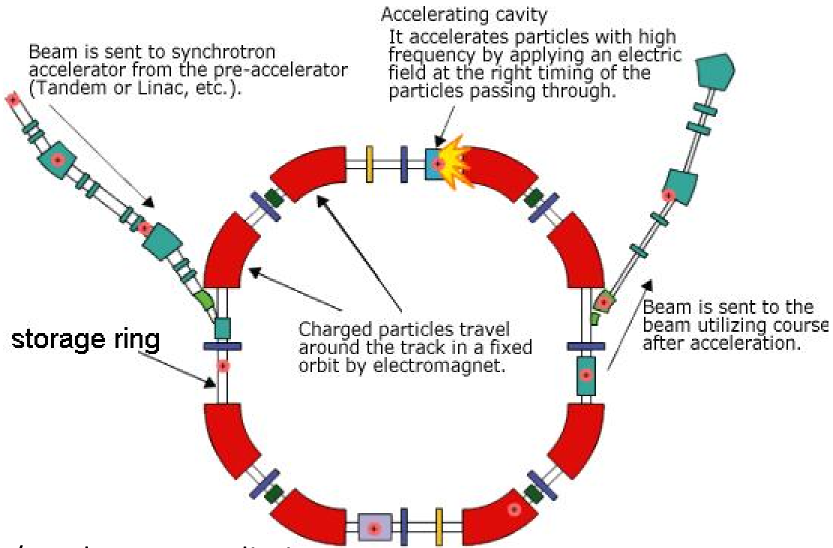

http://www.science20.com/mei/blog/synchrotron_radiation

Pulse structure at synchrotrons and cyclotrons

ISIS synchrotron. Pulsed beam: all protons (and muons) in one bunch

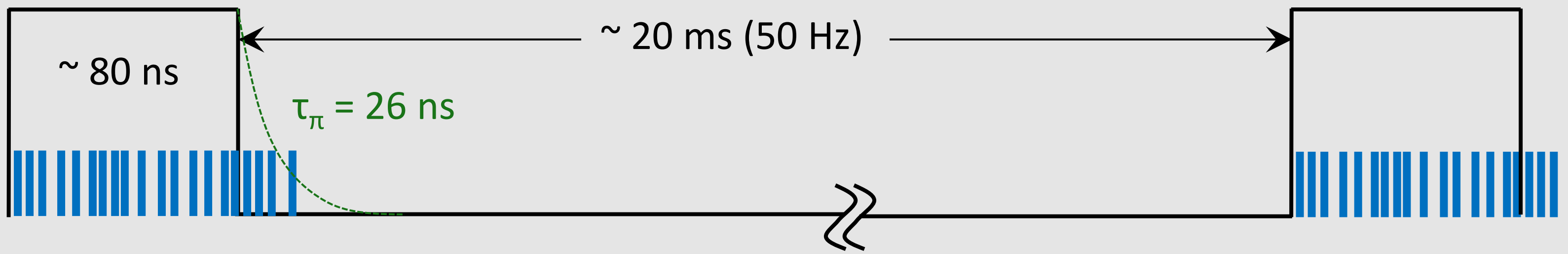

PSI 50 MHz Cyclotron. Continuous beam: muons arrive randomly

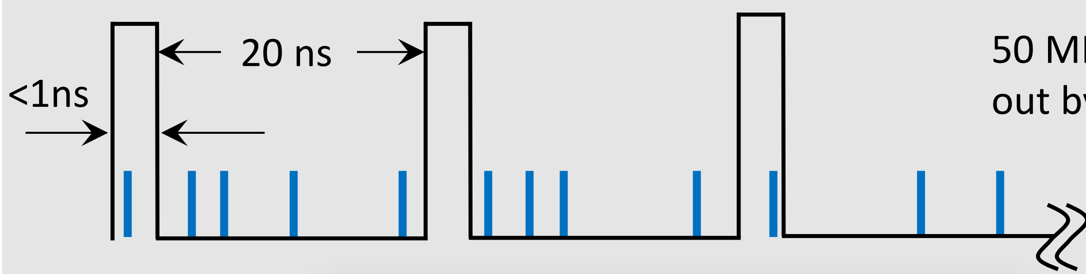

50 MHz time structure washed out by pion lifetime (26 ns)

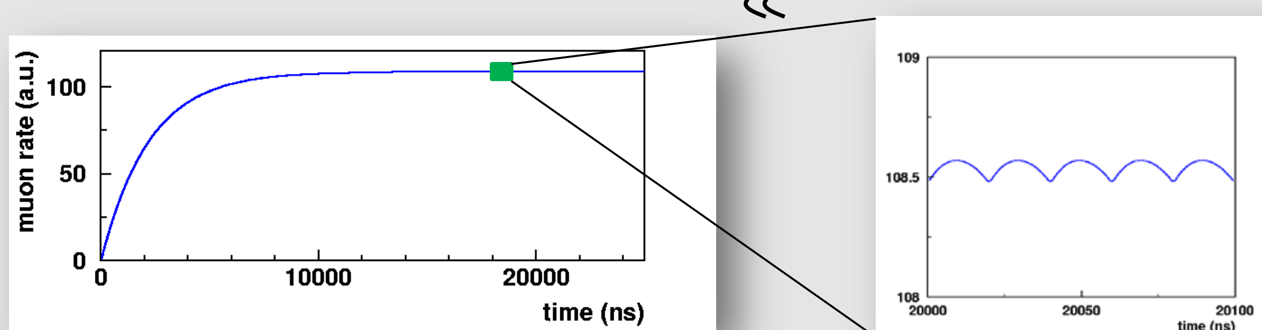

The PSI isochronous cyclotron

2.4 mA: ~1.5 x 10^{16} protons/sec @ 590 MeV:
1.4 MW on 5x5 mm^2 = 50 kW/mm^2, stainless steel melts in ~0.1 ms;
electric power demand of 3000 households

A MW proton beam allows to generate 100% polarized 4-MeV μ^+ beams with rates >10^8/sec

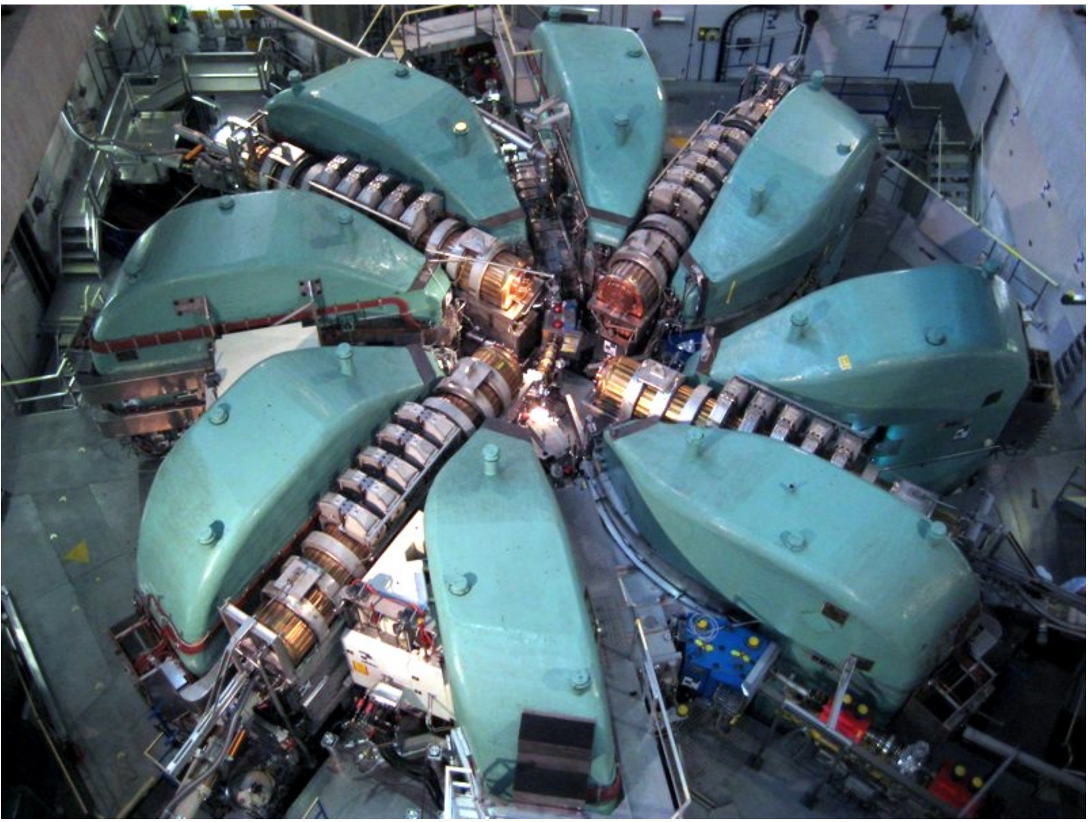

Larmor frequency of protons: $q/(2\pi m)$ = 15.25 MHz/T
$\boldsymbol{\nu_0 = q/(2\pi\gamma m)\cdot B,\ \gamma = E_{tot}/mc^2}$
$\boldsymbol{\nu_{rf} = n\cdot\nu_0}$, frequency of accelerating radio-frequency

Isochronous cyclotron: $\mathbf{B_0(R) \sim \gamma(R)}$, constant ν_{rf}!
PSI cyclotron: $\mathbf{B_0}$ = 0.554 T, $\boldsymbol{\nu_0}$ = 8.45 MHz, **n** = 6,
→ $\boldsymbol{\nu_{rf}}$ = 50.7 MHz

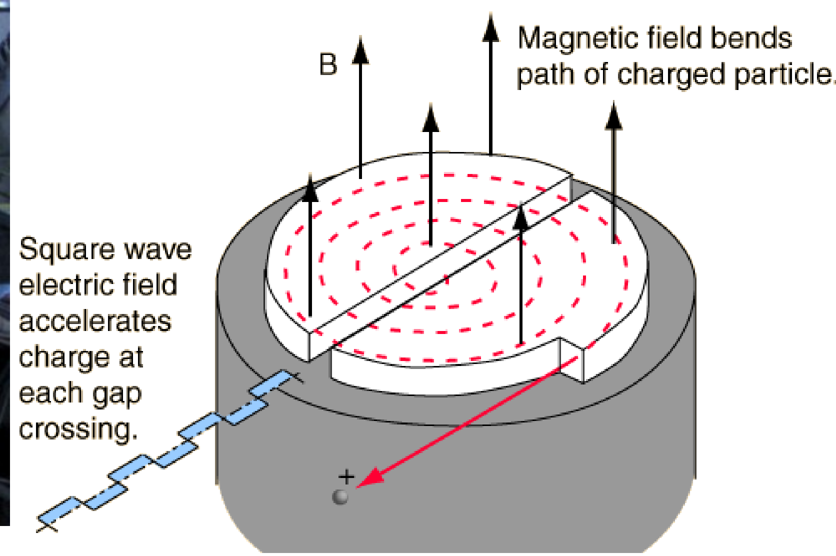

PSI muon beam time structure

Pion decay time of 26 ns is "smearing" the proton beam structure in the muon beam. This results in a "continuous" muon beam.

A μ^+ rate R of 10^5/s means: average time between two μ^+ is $1/R$ = 10 μs. Probability p to have ***the next*** μ^+ at time t:
$p = 1 - \exp(-Rt)$ ("pile-up", follows from Poisson statistics)

Single μ^+ can be detected with very good time resolution (< 0.1 ns), compared to a bunch width of 50-100 ns at pulsed beams. → measurement of GHz frequencies and fast relaxation rates (>100 μs^{-1}) possible. But "accidental" background in μ-decay histograms (can be reduced by muons-on-request).

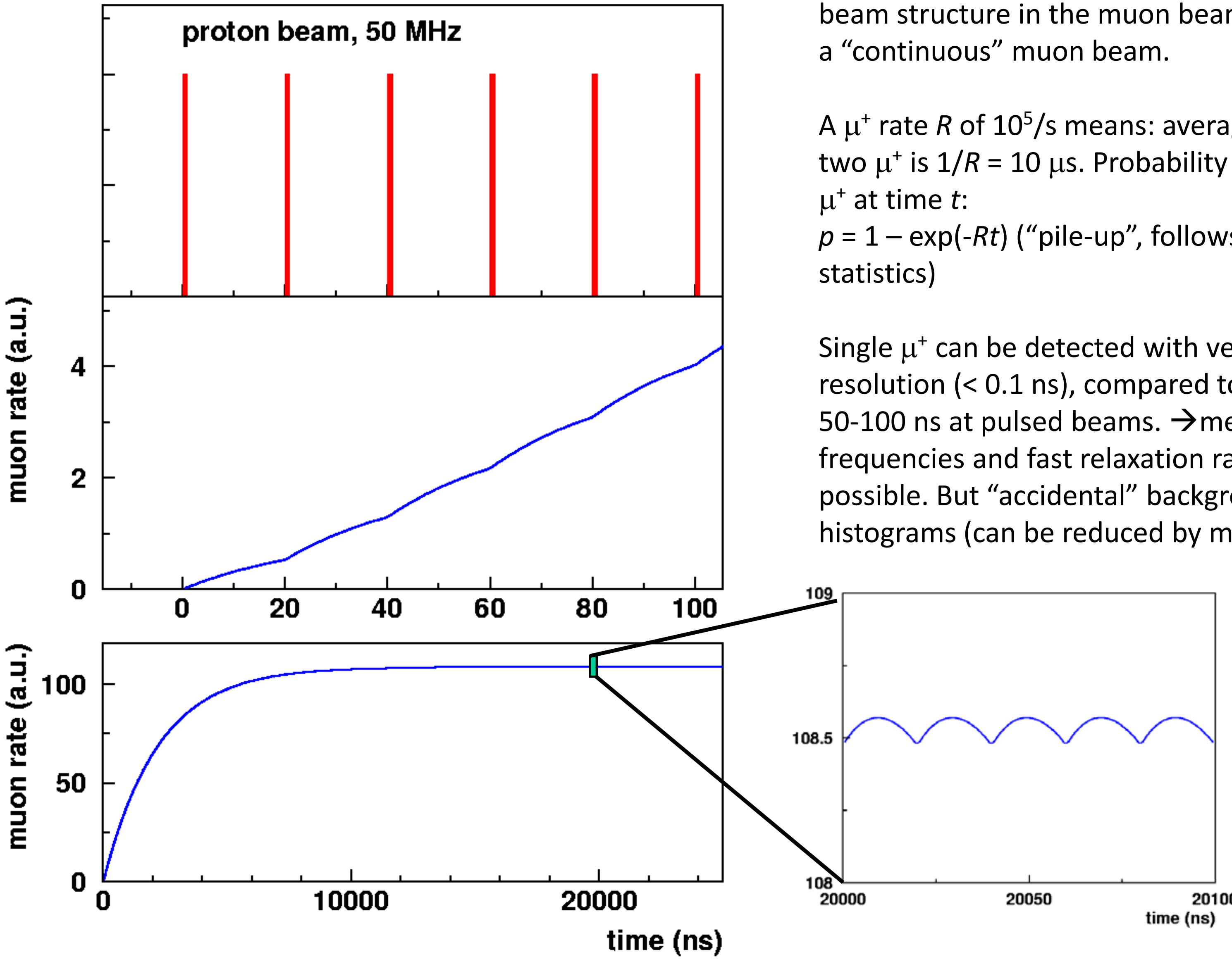

Continuous versus pulsed muon beams

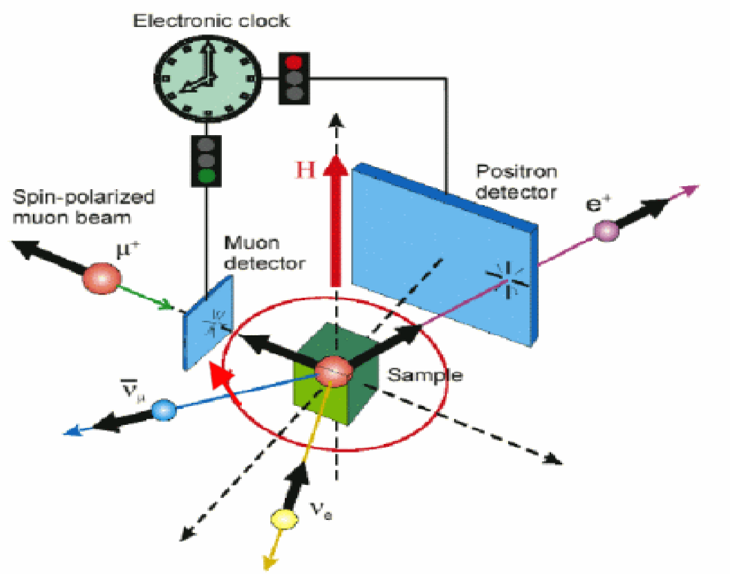

Figure 1. The transverse field μSR experiment. Drawing by Jeff Sonier, TRIUMF.

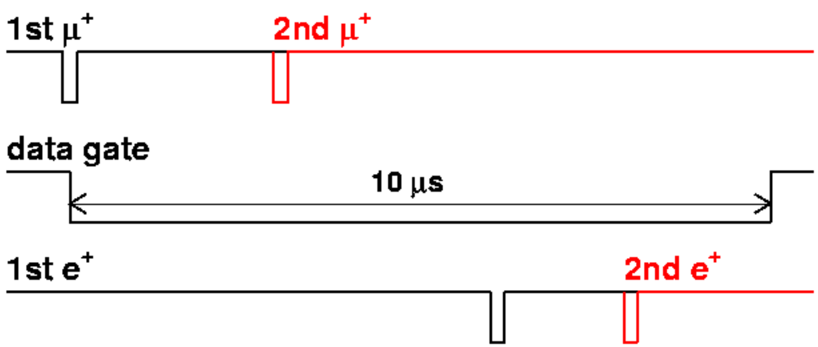

1st μ^+: there was no other μ^+ for at least 10μs in the past

Good Event = (data gate) • (1st e^+) • (no 2nd μ^+) • (no 2nd e^+)

$R_{acc} = R_\mu \times \exp(-2\Delta t\, R_\mu)$, $\Delta t = 10\ \mu s$

background due to uncorrelated detector hits $\mathrm{bkg(bin)} \cong N_{DataGates}\, t_{bin} * R_{e+}$

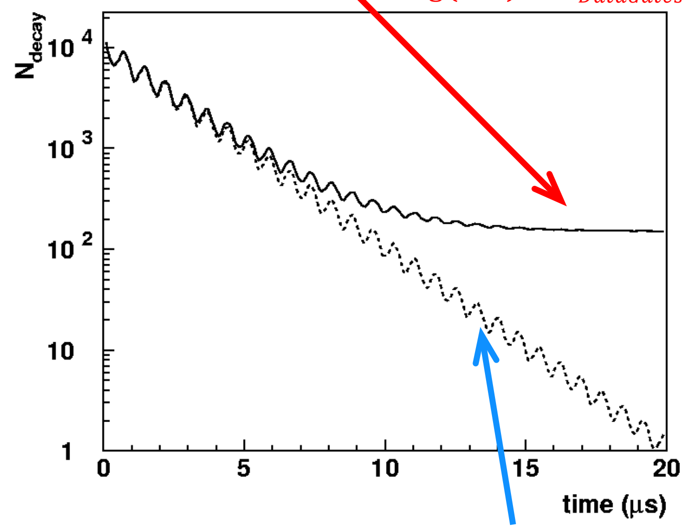

Low background at a pulsed beam

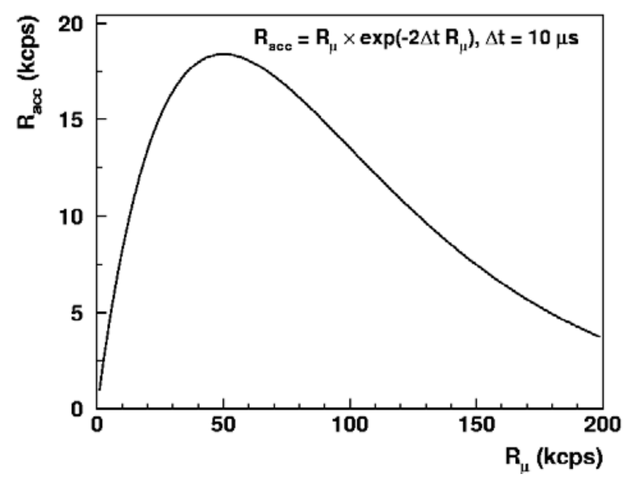

Continuous versus pulsed muon beams

Observable asymmetry $A(\omega)$ as a function of time resolution σ_t:

$$\mathbf{A(\omega) = A_0 \times \exp(-\omega^2\sigma_t^2/2)}$$

Continuous beam: σ_t < 300 ps

Pulsed beam: σ_t ~ 50ns

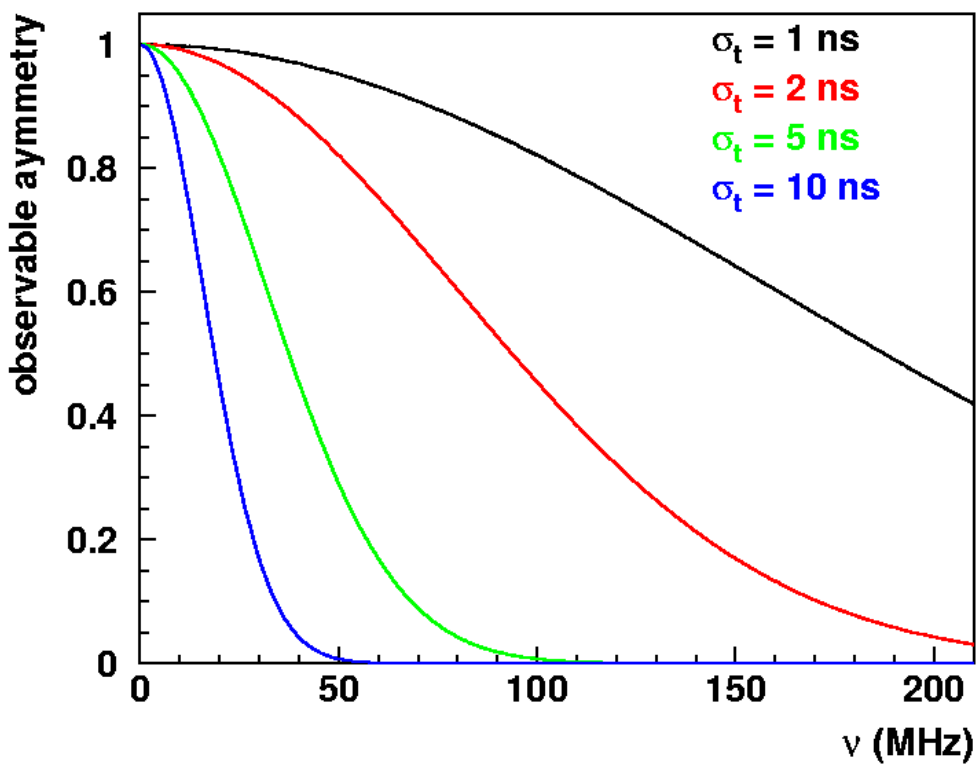

Continuous versus pulsed muon beams

continuous
muon beams

No need of high detector segmentation

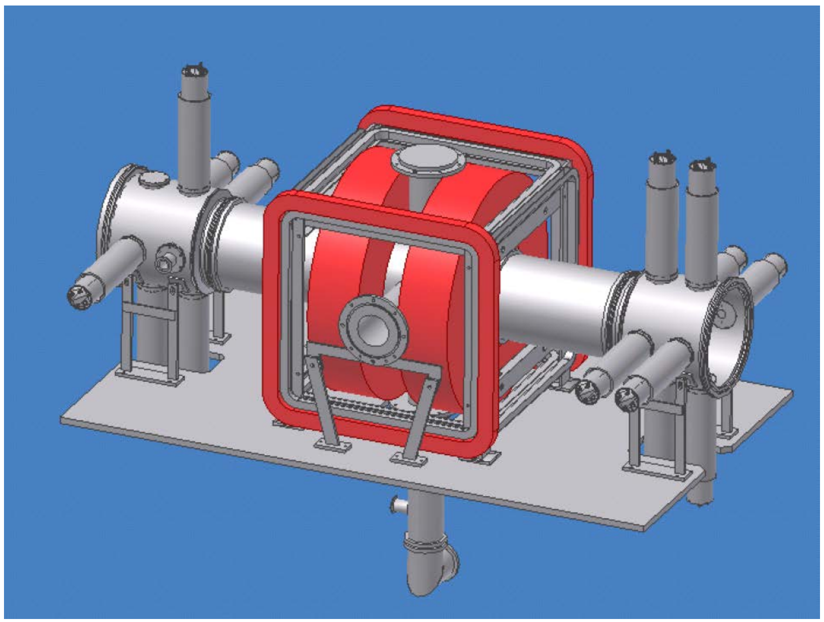

Example: "GPS" instrument at PSI
1 backward + 1 forward detectors

pulsed (50Hz)
muon beams

High detector segmentation mandatory

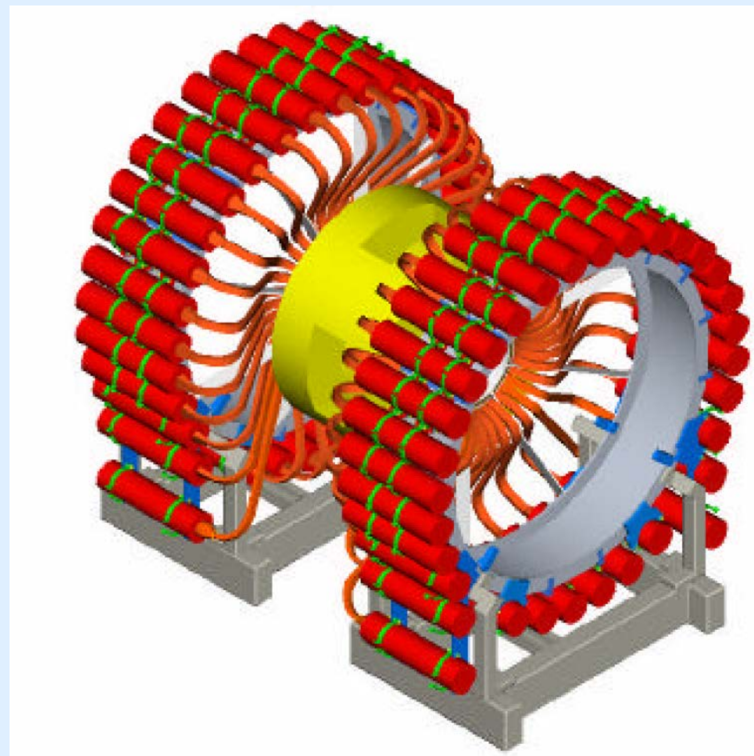

Example: "MuSR" instrument at ISIS
32 backward + 32 forward detectors

Continuous versus pulsed muon beams

continuous muon beams

"Continuous Wave (CW)"

- **No distinct time structure**
- **Each muon individually counted.**
  "Start" signal (muon detector)
- **Very good time resolution**
  (< 100 ps possible)
  - **Detection of large magnetic fields**
  - **Detection of fast relaxing signals**
- **Reduction of muon rate to avoid "pileup"**
- **Non-negligible background (bkg), limited time window (10μs typically); bkg can be reduced by Muons-On-REquest (MORE), time window expanded.**

pulsed (25 Hz or 50Hz) muon beams

- **Distinct time structure**
  (pulse structure of proton beam)
- **All muons coming at (almost) the same time.**
  No need of muon detector.
  (Pulse width 10ns – 100ns)
- **Very low background (possibility to measure slow depolarization rates)**
- **Limited time resolution**
  - **Detection of large magnetic fields and/or fast relaxing signals <u>impossible</u>**
- **High instantaneous rates requires very high detector segmentation**

Muons On Request (MORE) to suppress background

- GPS “tells” kicker to send a muon to GPS
- If a muon is detected in GPS “tell” kicker to send the beam to LTF
- no random beam background in GPS
- if decay e^+ is detected in GPS the next muon is requested from the kicker

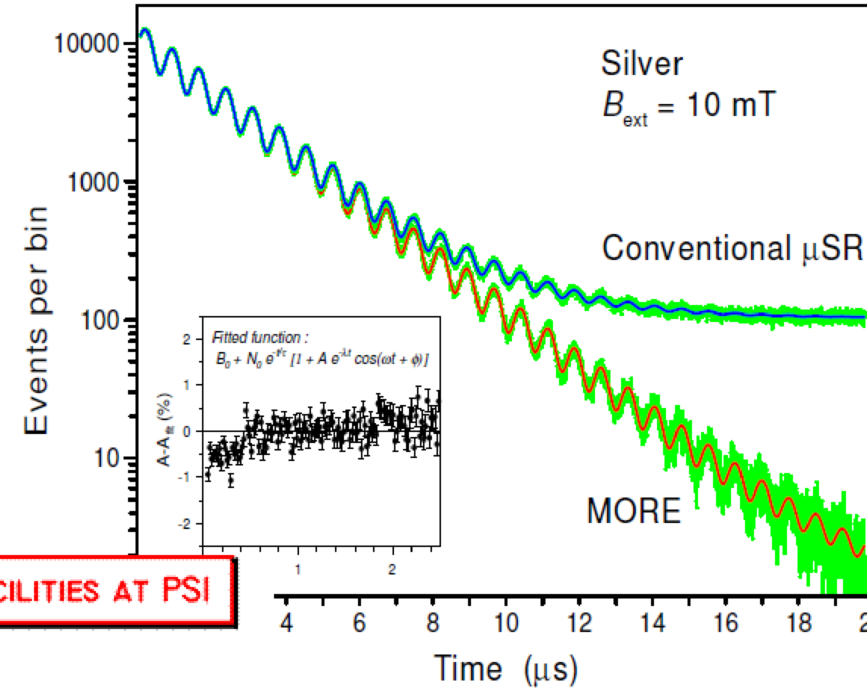

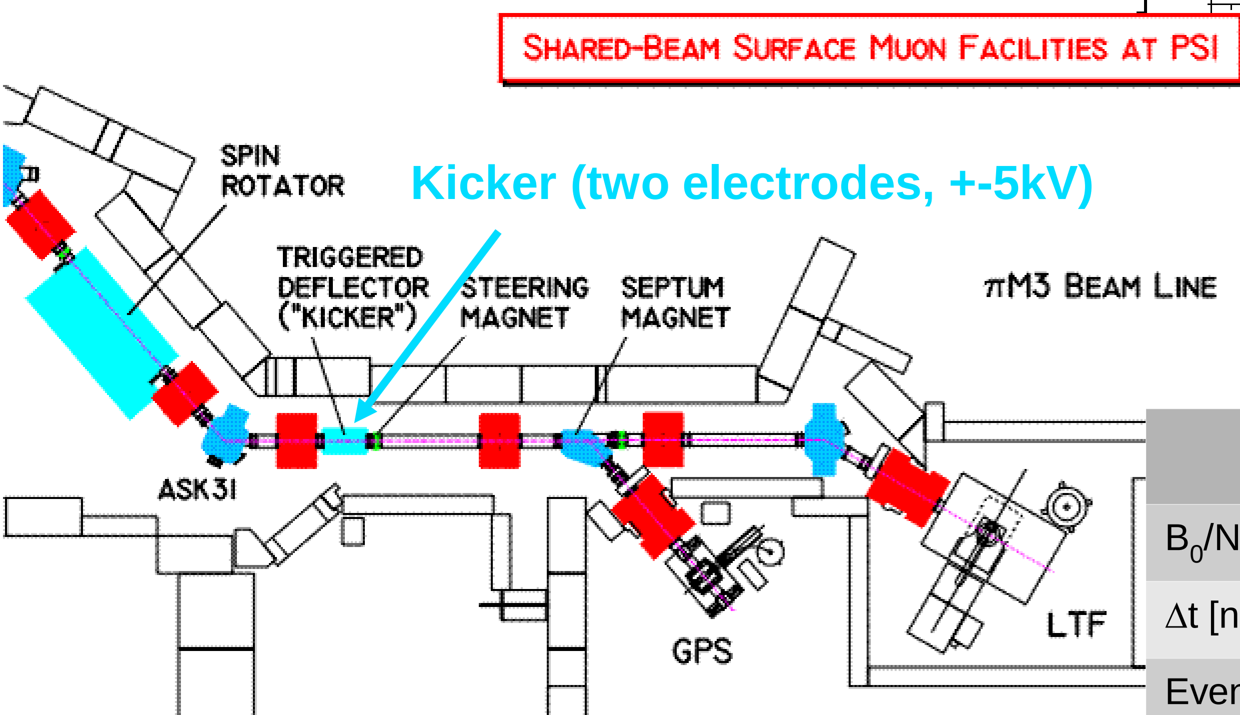

	“normal”	MORE	pulsed
B_0/N_0 [10^{-5}]	660	9	1
Δt [ns]	<1	<1	80
Events [10^6/h]	12	20	200

Muon beams at SμS

"Arizona" or "Surface Muon Beam" (only μ^+), ~100% polarization

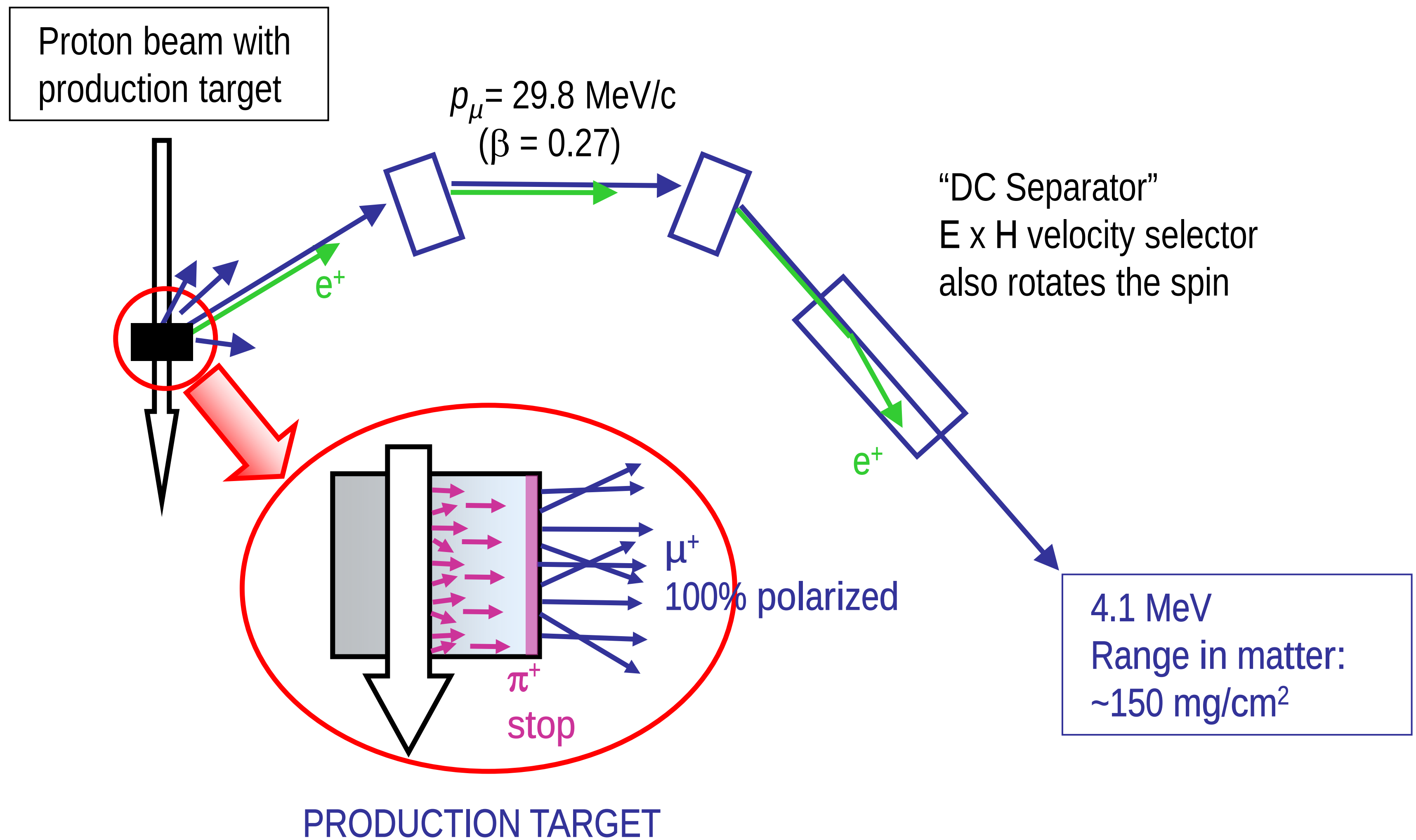

Muon beam at SμS

(Traditional) "Decay Muon Beam" (μ^+ or μ^-), ~80% polarization

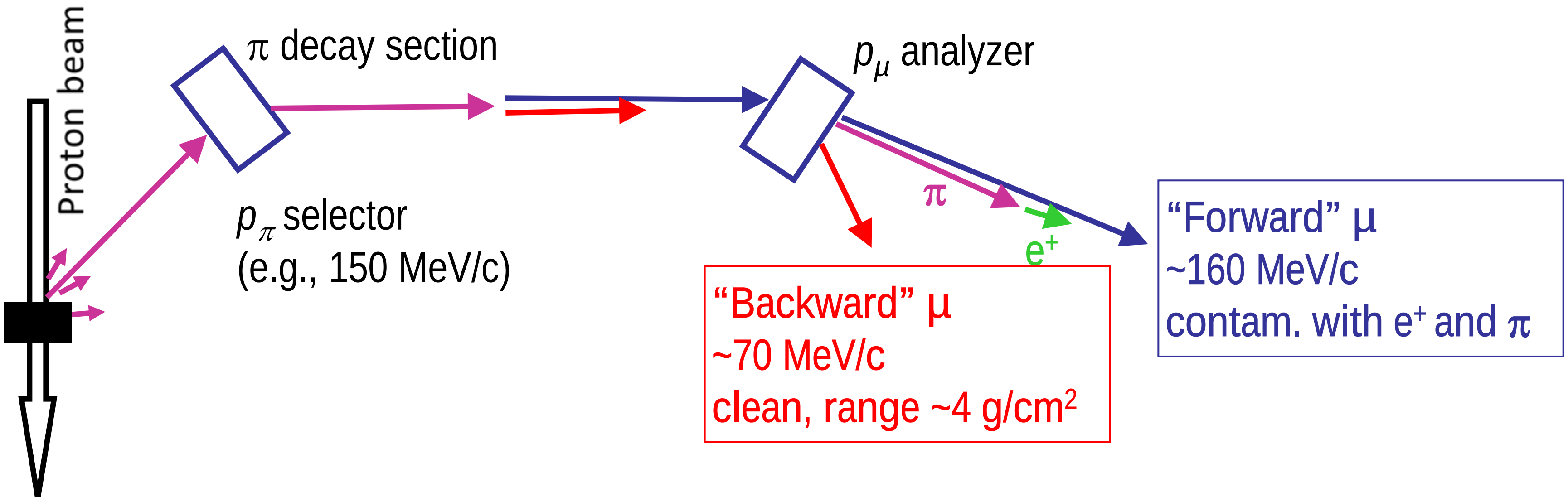

to select beam momentum *p*: magnetic dipole magnets (bending magnets)

to focus beam: magnetic quadrupole dublets or triplets, solenoids (for «surface muons»)

to vary beam intensity, momentum width *Δp/p*: slits

to remove positrons from beam, to rotate muon spin (for «surface muons» only):
ExB velocity filter (separator, spin-rotator)

Muon instruments at SμS (Swiss Muon Source)

590MeV 2.4 mA

HAL-9500

High Field and Low Temperature, μ^+ energy: **4 MeV**

9.5 T

10 mK – 300 K

GPS

General Purpose Surface Muon Instrument

Muon energy: **4 MeV** (μ^+)

0.6 T, 1.6 - 1000 K

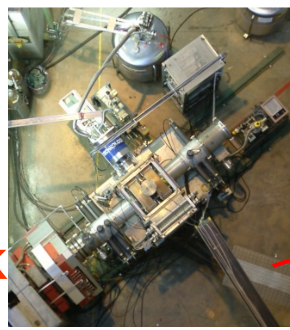

Shared Beam Surface Muon Facility (Muon On REquest)

LTF

Low Temperature Facility

Muon energy: **4 MeV** (μ^+)

3 T, 20 mK- 4 K

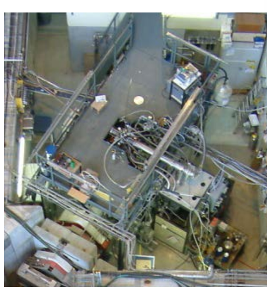

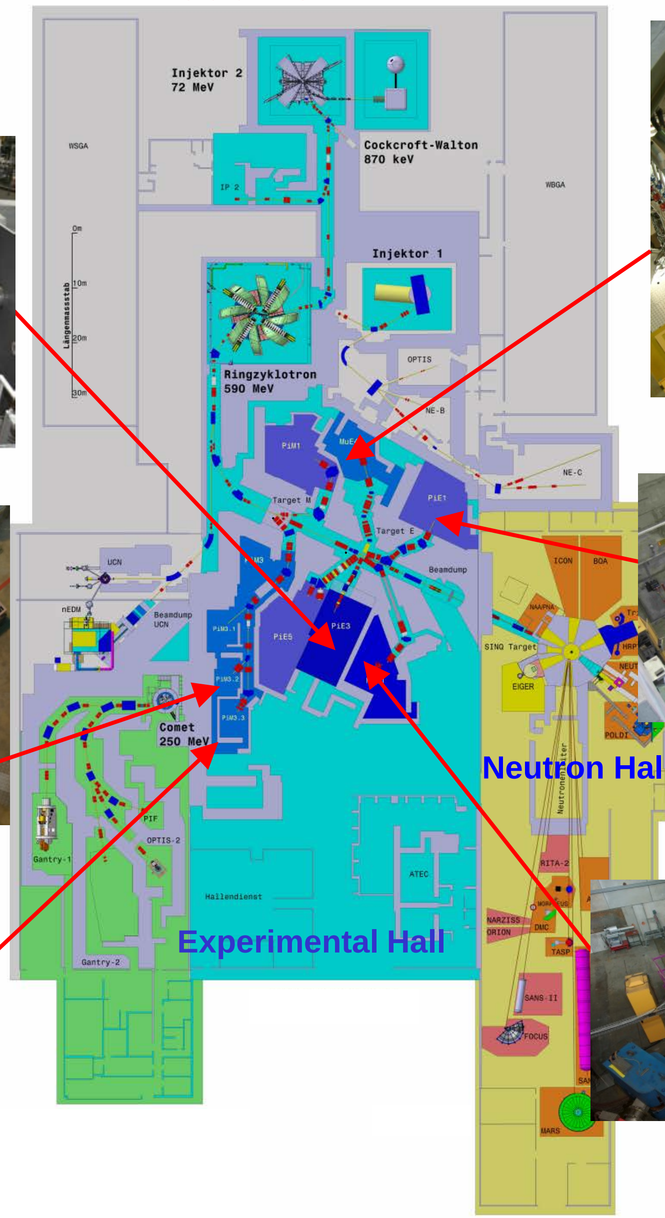

LEM

Low-energy muon beam and instrument, tunable energy (**1-30 keV**, μ^+), *thin-film, near-surface and multi-layer studies*

(5-200 nm)

0.34 T, 2.3 - 600 K

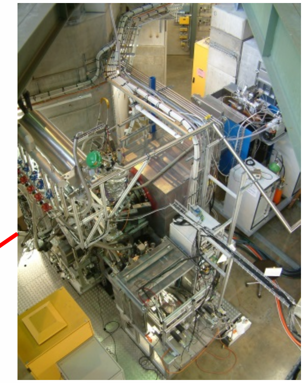

DOLLY

General Purpose Surface Muon Instrument

μ^+ energy: **4 MeV**

0.5 T, 0.25 – 300 K

GPD

General Purpose Decay Channel Instrument Pressure studies

Muon energy: **5 - 60 MeV** (μ^+ or μ^-)

0.6 T, 0.3 – 300 K, 2.8 GPa

Muon Production – Example: Target E at PSI

- Rotating Graphite Target (1 Hz)
- Radiation Cooled, T_{avg} = 1700K
- Thickness t=40 mm; h=6 mm; ∅ 450 mm
- Radiation Losses 30%

$p + C \rightarrow \pi^+ \pi^- p\ n \ldots$

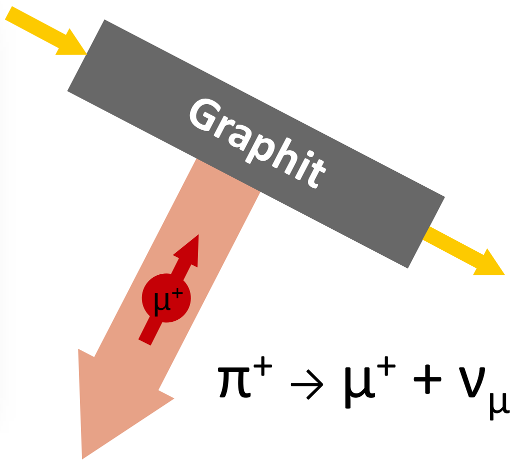

$\pi^+ \rightarrow \mu^+ + \nu_\mu$

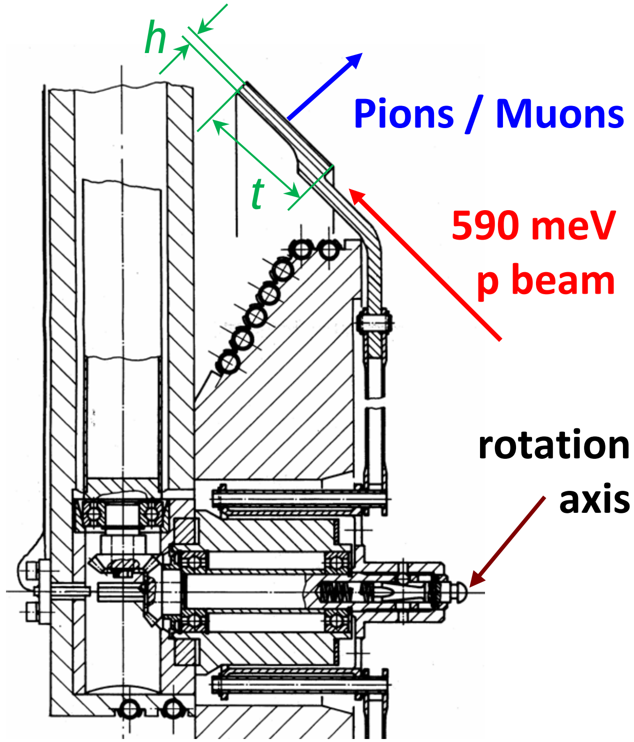

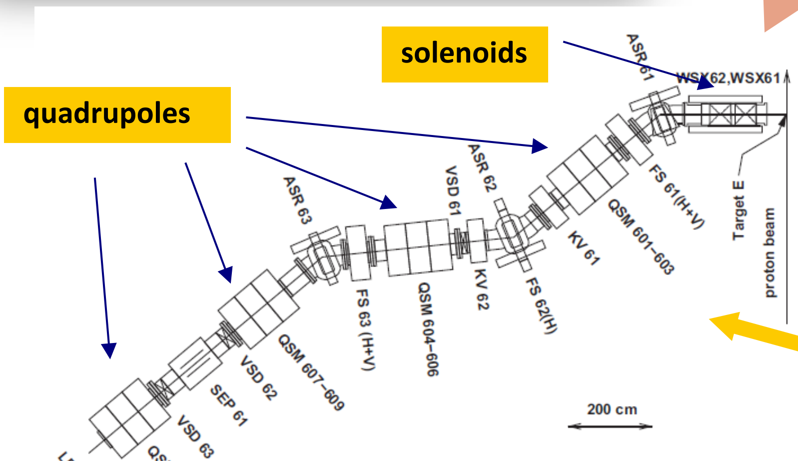

T.Prokscha *et al* NIM-A (2008)

2400 μA ≈ 1.5·10^{16} p/sec @ 590MeV →
≈ 10^7 – 10^8 μ$^+$/sec,
≈ 100% polarized (surface muons: ≈ 4 MeV)

μE4 beamline at PSI: 5 · 10^8 μ$^+$/sec
(highest intensity muon beam in the world)

PAUL SCHERRER INSTITUT

How to generate a low-energy μ^+ beam with tunable energies between 1 and 30 keV?

Muons are born energetically in pion decay (~4 MeV)

Need a special moderation technique to slow down energetic muons from the MeV to keV energies

Range of muons in matter

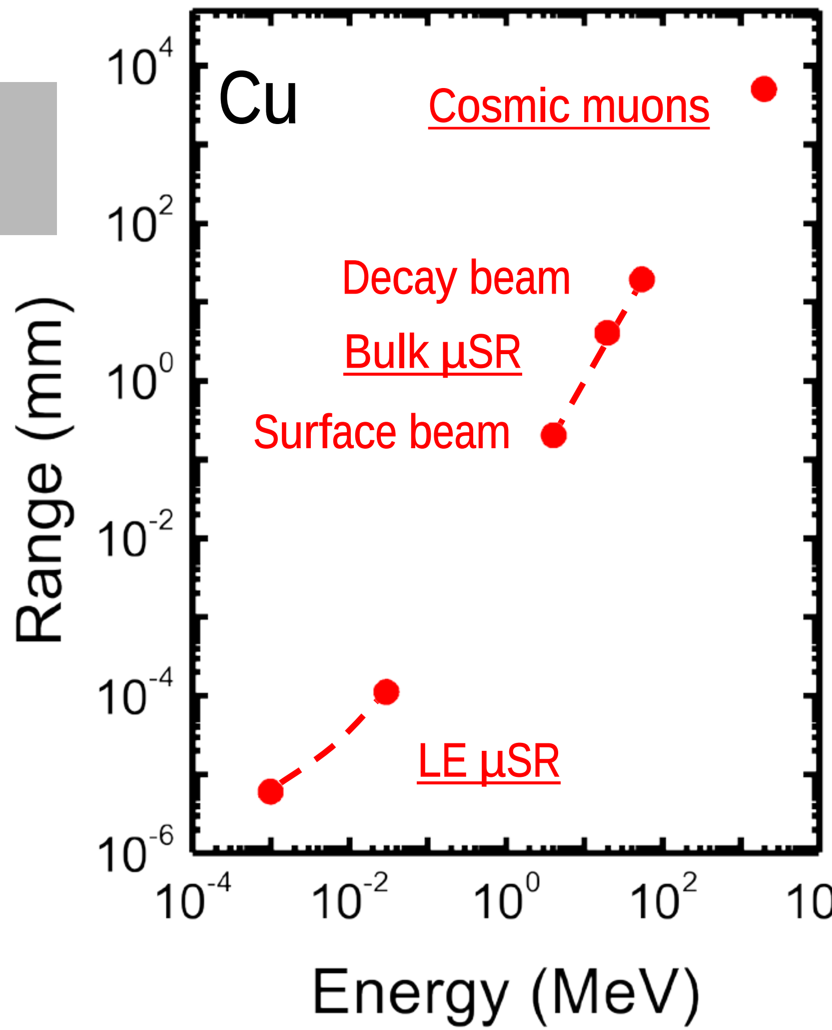

Accelerator muons:

- "**decay beam**", pions decaying in flight: muon energies $\mathbf{E_{\mu}}$ = 5 – 80 MeV
- "**surface muon beam**", pions decaying at rest at surface of production target: $\mathbf{E_{\mu}}$ <= 4.1 MeV
- "**low energy muon beam**" ($\mathbf{E_{\mu}}$ < 30 keV), moderation of a surface muon beam

Bulk μSR:

▶ "Normal" samples (sub-mm), bulky samples + samples in containers or pressure cells

Low-Energy μSR (LE-μSR) (< 30 keV):

▶ Depth-selective investigations (1–200 nm)

Generation of thermal μ^+ at a pulsed accelerator

VOLUME 74, NUMBER 24 PHYSICAL REVIEW LETTERS 12 JUNE 1995

Ultraslow Positive-Muon Generation by Laser Ionization of Thermal Muonium from Hot Tungsten at Primary Proton Beam

K. Nagamine,[1,2] Y. Miyake,[1] K. Shimomura,[1] P. Birrer,[1] J. P. Marangos,[1,3] M. Iwasaki,[1] P. Strasser,[2,4] and T. Kuga[5]

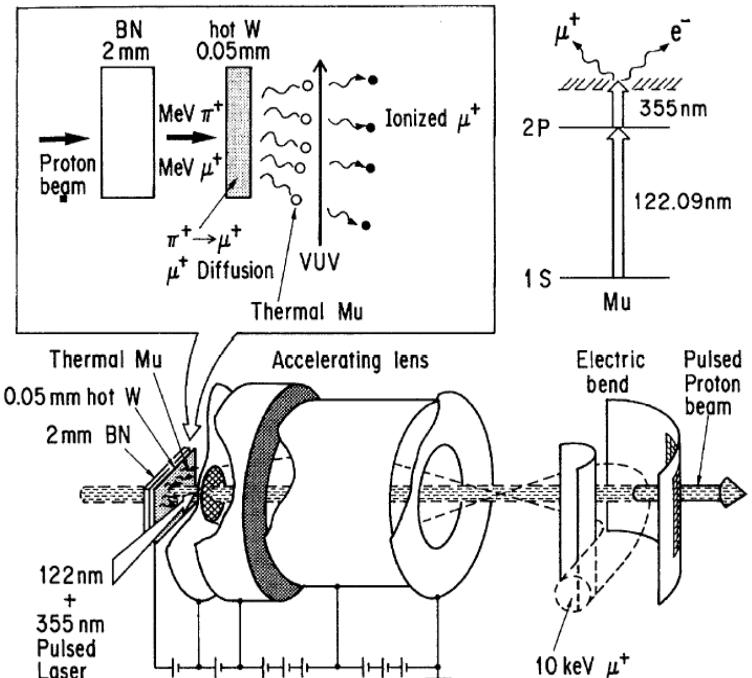

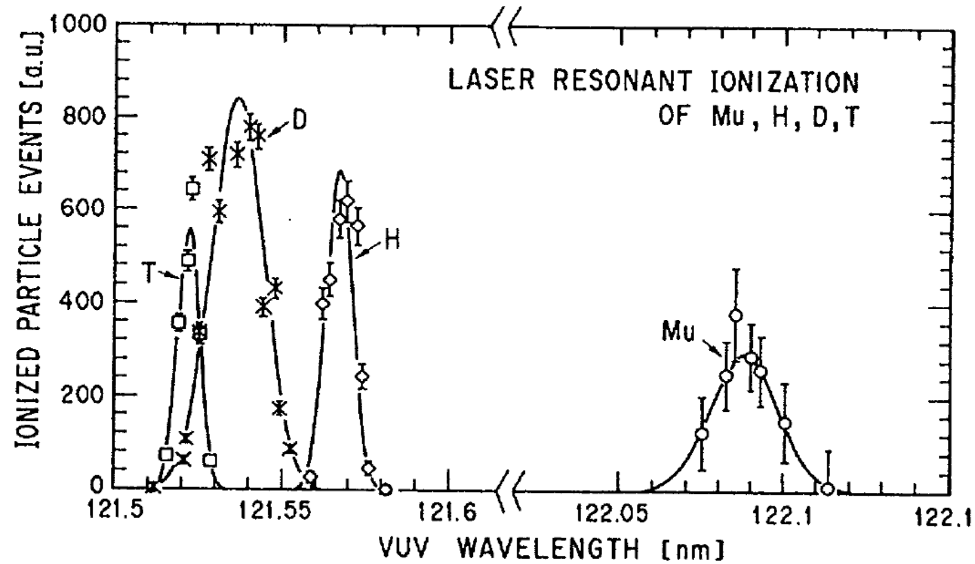

P. Bakule,Y.Matsuda,Y.Miyake, K. Nagamine, M. Iwasaki, Y. Ikedo, K. Shimomura, P. Strasser, S. Makimura, Nucl. Instr Meth. B **266**, 335 (2008).

Pulsed LE-μ^+ beam (25Hz) @ ISIS/RIKEN-RAL and J-PARC:

Intensity: ~15 LE-μ^+/sec (>10^3/s at J-PARC expected)
Polarization: ~ 50% (1/2 of polarization lost in muonium)

Generation of polarized epithermal (~eV) μ^+

„Surface“ Muons

~ 4 MeV

~ 100% polarized

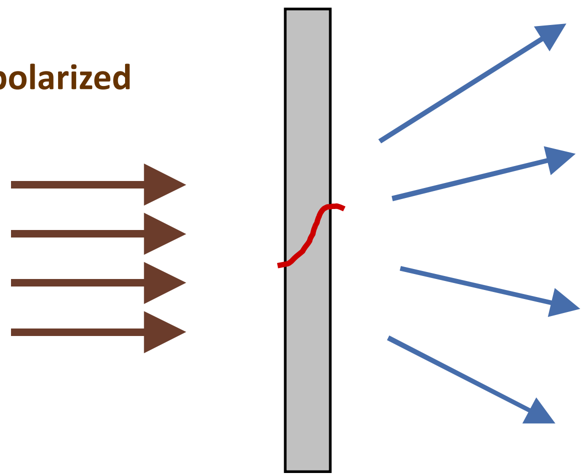

~100 μm Ag

Energy spectrum after a degrader

Solid line: muon energy spectrum

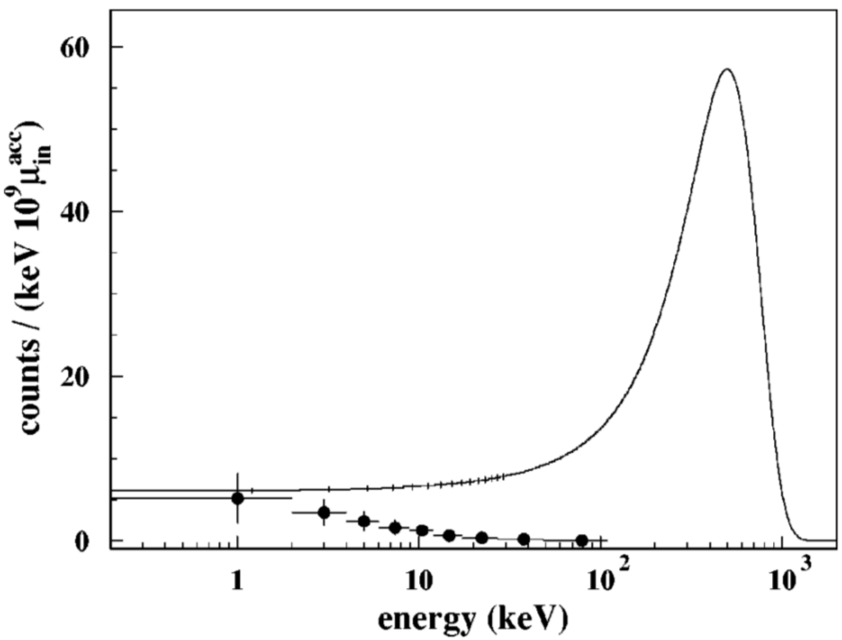

Using a proper moderator:

motivated by experiments for positron moderation, a solid film of a rare-gas should work!

T. Prokscha et al., Phys. Rev. **A58**, 3739 (1998).

Generation of polarized epithermal (~eV) μ^+

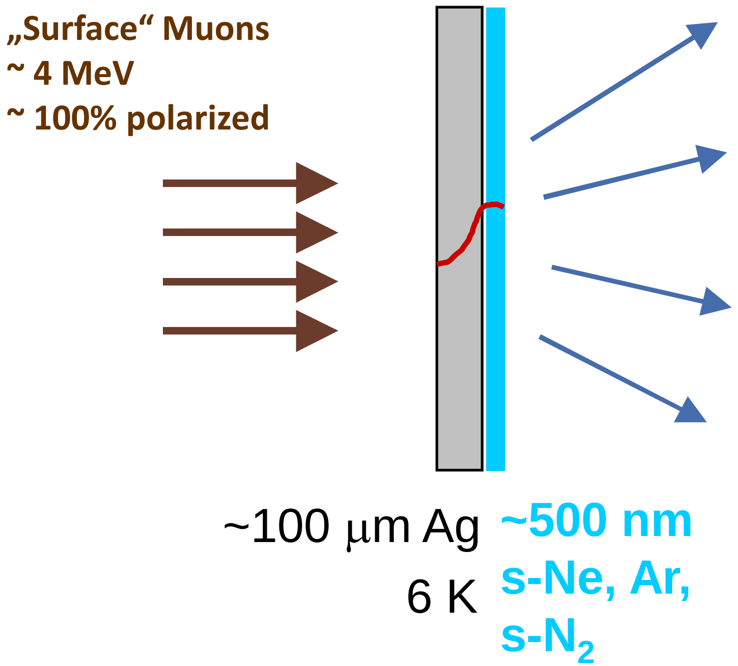

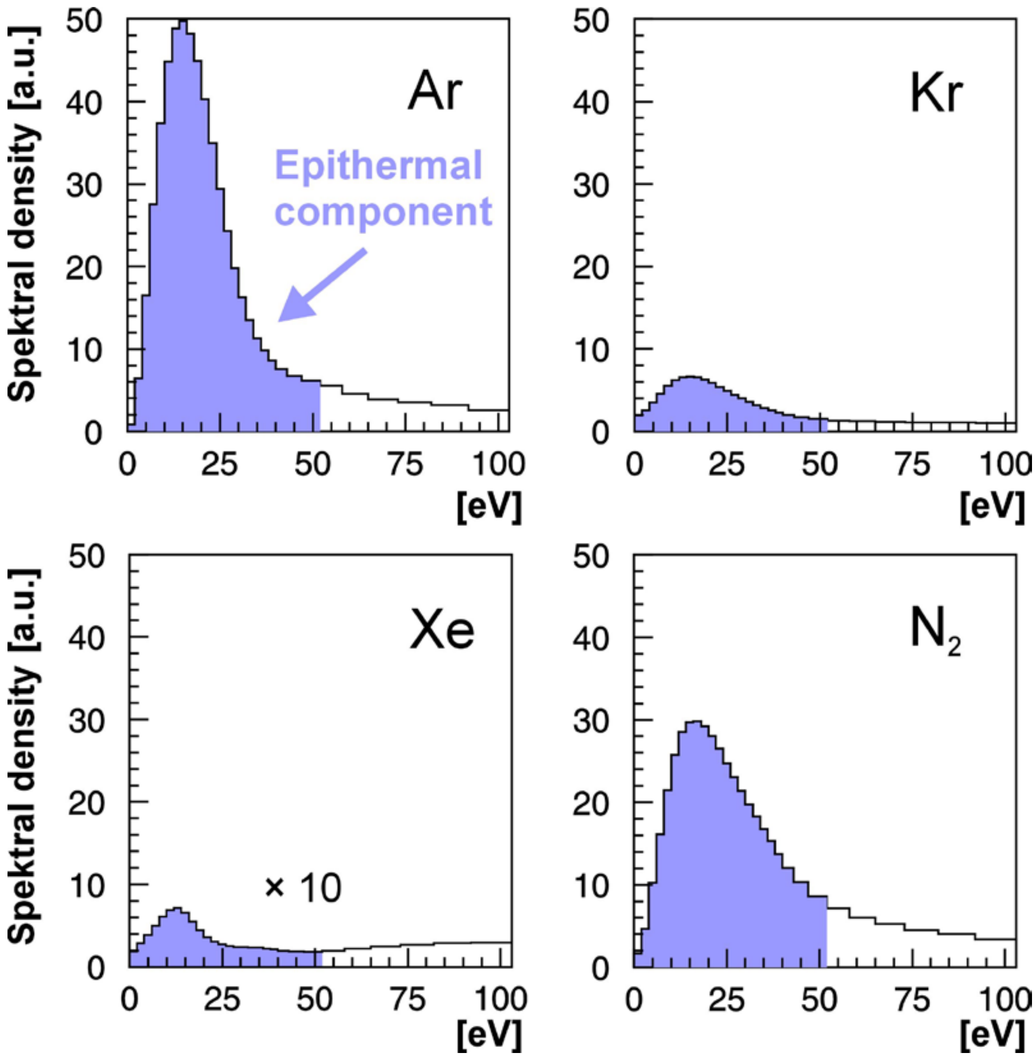

T. Prokscha et al., Appl. Surf. Sci. **172**, 235 (2001).
T. Prokscha et al., Phys. Rev. **A58**, 3739 (1998).
E. Morenzoni et al., J. Appl. Phys. **81**, 3340 (1997).
D. Harshmann et al., Phys. Rev. **B36**, 8850 (1987).

Characteristics of epithermal (~eV) μ^+

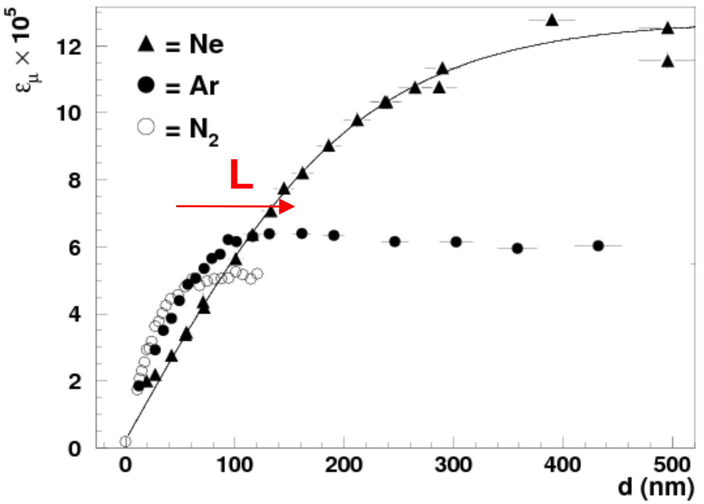

E. Morenzoni, T. Prokscha, A. Suter, H. Luetkens, R. Khasanov, J.Phys.: Cond. Matt. **16**, S4583 (2004).

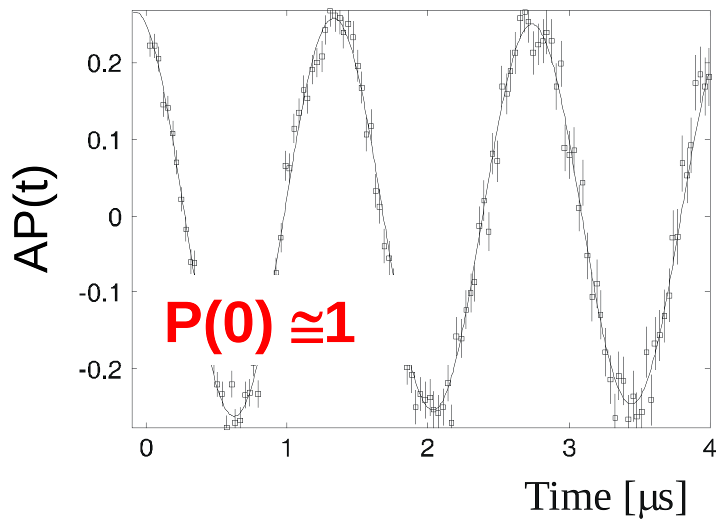

E. Morenzoni, F. Kottmann, D. Maden, B. Matthias, M. Meyberg, T. Prokscha, T. Wutzke, U. Zimmermann, PRL **72**, 2793 (1994).

→ suppression of electronic energy loss for $E > E_g$, large band gap E_g (10-20 eV) „soft, perfect“ insulators

→ large escape depth L (10-100 nm), no loss of polarization during moderation (~10 ps)

→ **moderation efficiency is low (requires highest intensities μ^+ beams, > 10^8 μ^+/s, i.e. MW proton beam):**

$$\boldsymbol{\varepsilon_{\mu+} = N_{epith}/N_{4MeV} \approx \Delta\Omega\,(1-F_{Mu})\,L/\Delta R \approx 0.25\,L/\Delta R \approx 10^{-4} - 10^{-5}}$$

$\Delta\Omega$: probability to escape into vacuum (~50% for isotropic angular distribution)
F_{Mu}: muonium formation probability

Low-energy (keV) μ^+ facility and LE-μSR setup

Rates are for 6-cm target E and 1.8 mA proton current (2017)

- UHV system, 10^{-10} mbar
- some parts LN_2 cooled

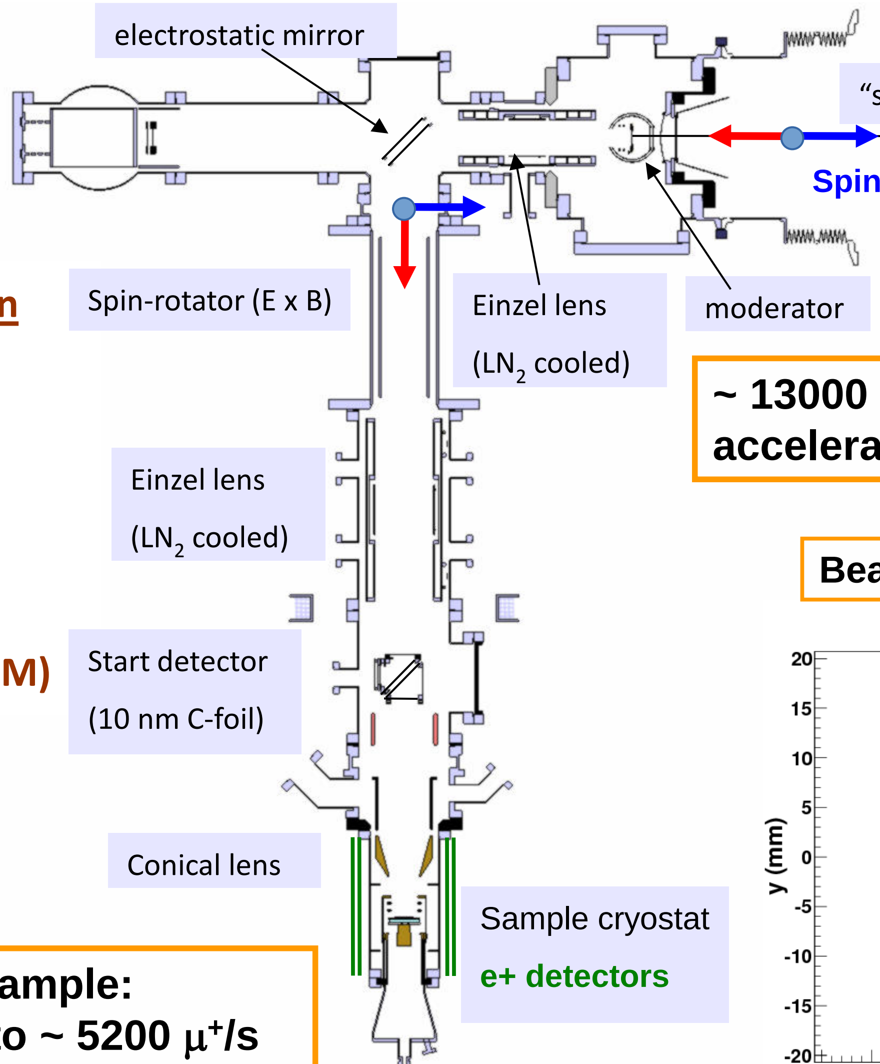

~2.2 • 10^8 μ^+/s

~ 13000 LE-μ^+/s; accelerate up to 20 keV

Polarized Low Energy Muon Beam

Energy: 1-30 keV

ΔE, Δt: 400 eV, 5 ns

Depth: 1 – 200 nm

Polarization ~100 %

Beam Spot: 12 mm (FWHM)

Sample environment:

B = 0 – 0.34 T $\perp$,
0 – 0.03 T $\parallel$ sample
T = 2.2 – 600 K

at sample:
up to ~ 5200 μ^+/s

Beam spot at sample

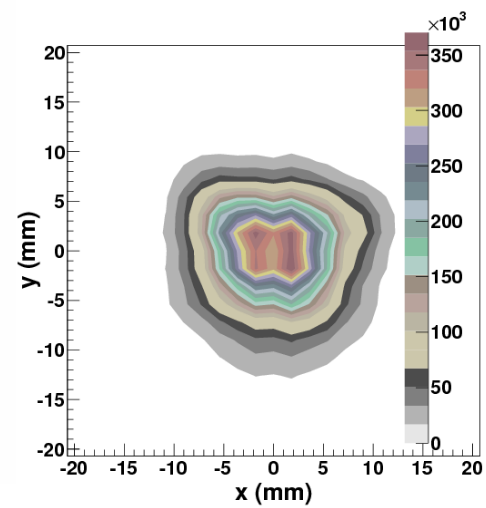

Low-energy (keV) μ⁺ facility and LE-μSR setup

Muon Spin
Muon Momentum

Spin-Rotator / Separator

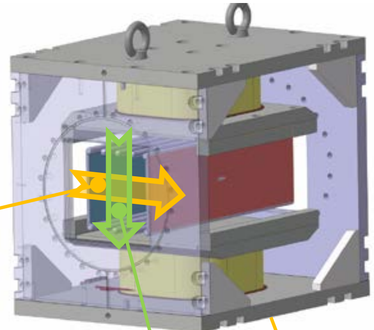

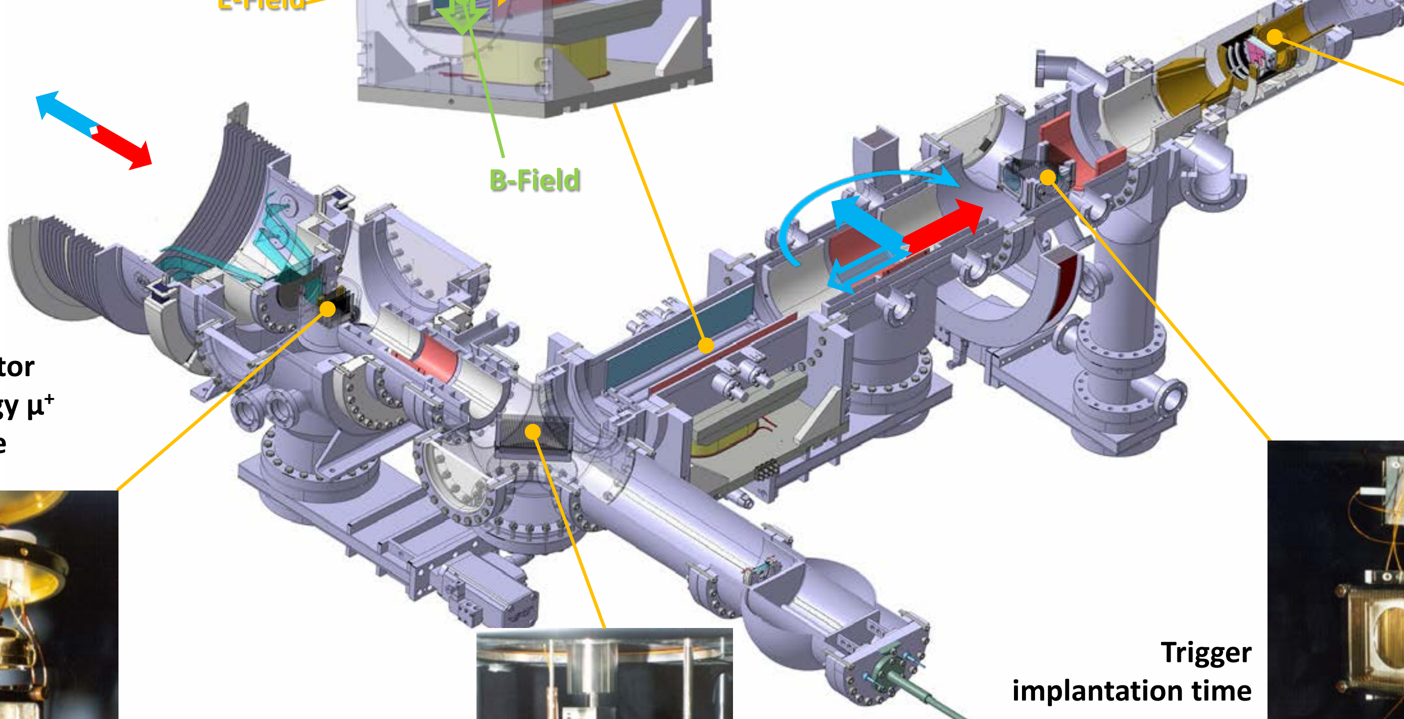

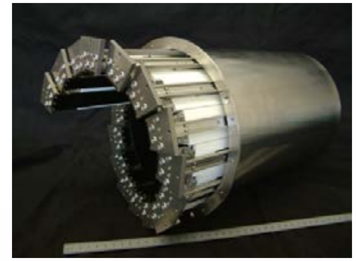

APD Positron Spectrometer

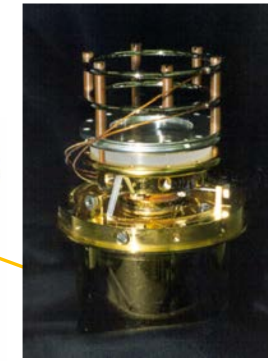

Sample Cryo

Moderator low energy μ^+ source

Mirror energy filter

Trigger implantation time

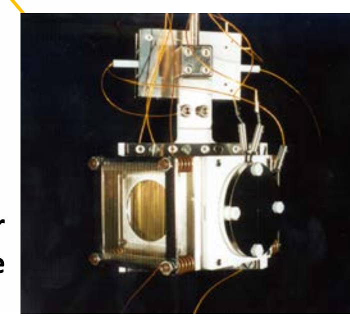

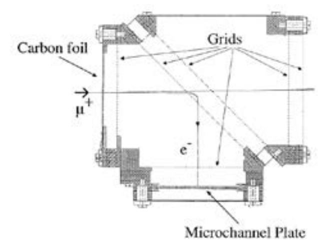

Low-energy μ^+ facility (LEM) at μE4 beam line

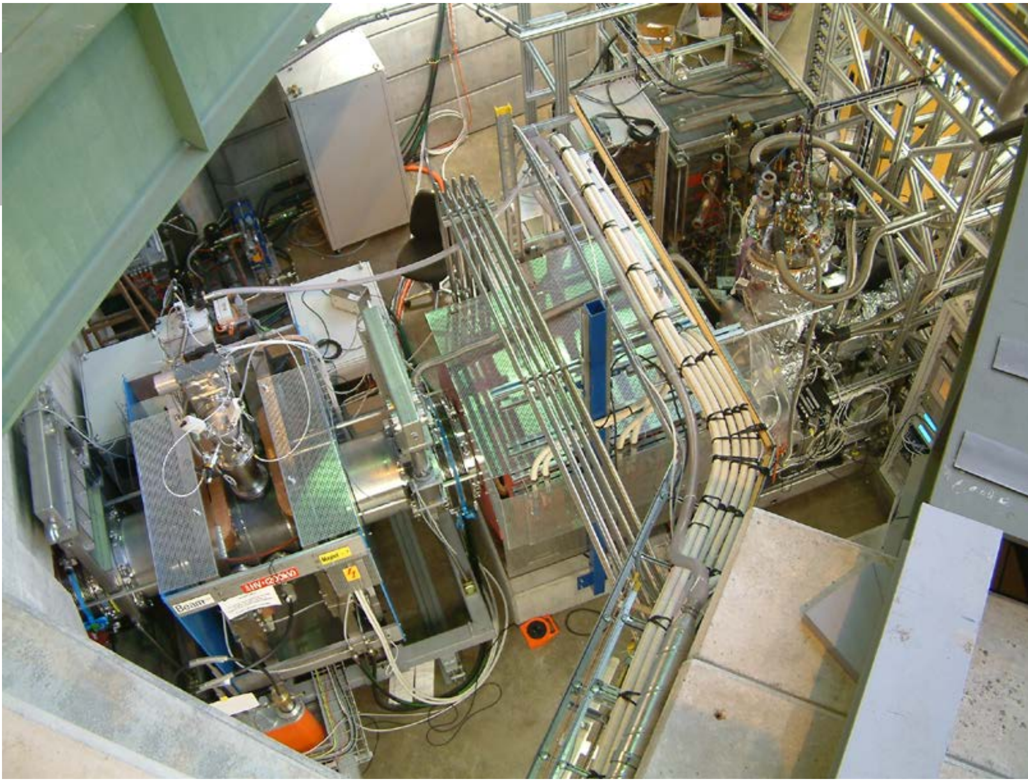

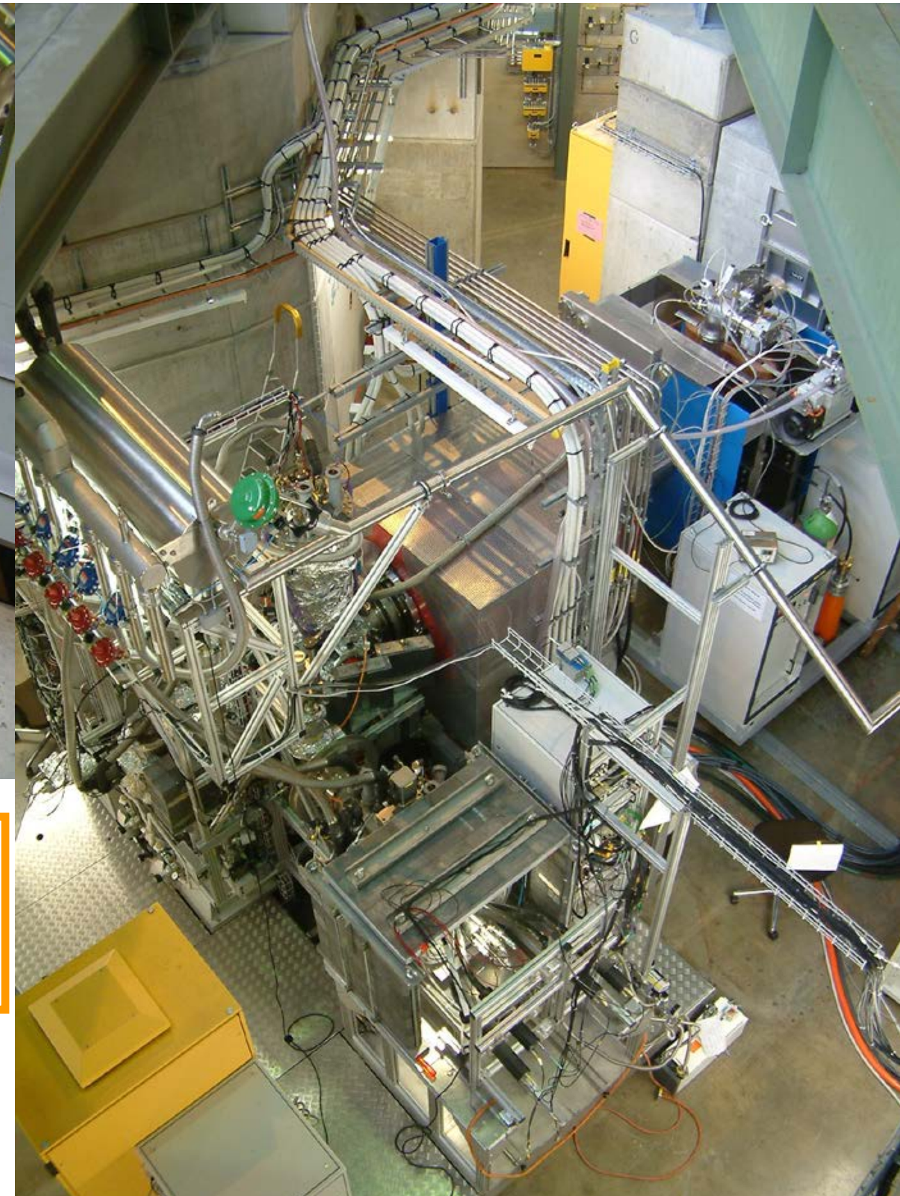

At 2.4 mA proton current (4-cm target E):

5 • 10^8 μ^+/s total, $\Delta p/p$ = 9.5% (FWHM) ~2.1 • 10^8 μ^+/s on LEM moderator ~1.2 • 10^4 μ^+/s moderated (solid Ar)

T. Prokscha, E. Morenzoni, K. Deiters, F. Foroughi, D. George, R. Kobler, A. Suter and V. Vrankovic, Nucl. Instr. Meth. **A595**, 317 (2008).

Implantation profiles of low-energy muons

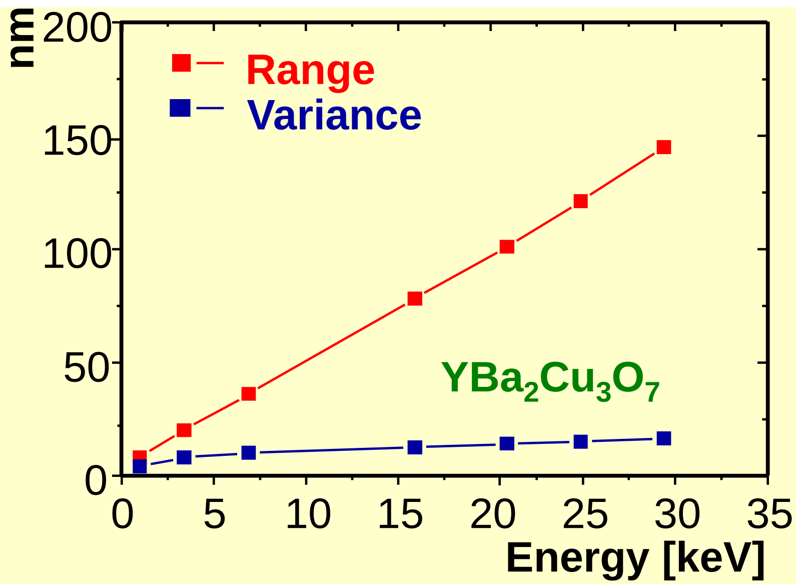

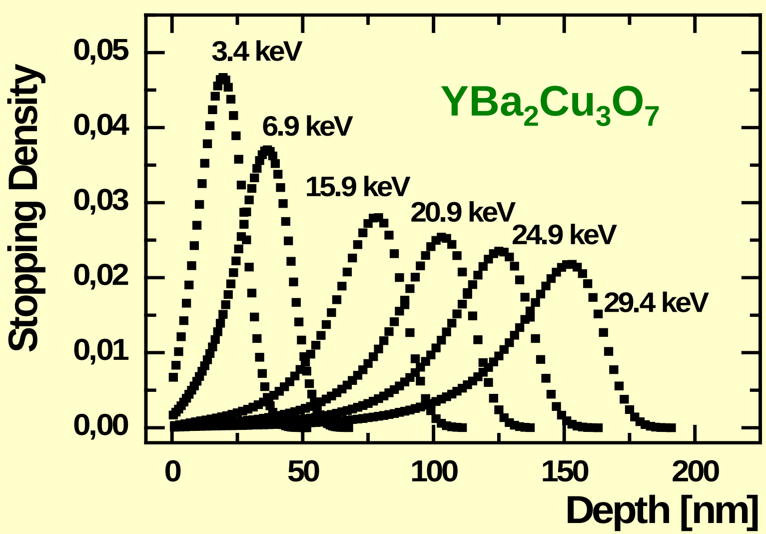

Stopping profiles calculated with Monte Carlo code Trim.SP by W. Eckstein, MPI Garching, Germany.

Experimentally tested for muons

E. Morenzoni, H. Glückler, T. Prokscha, R. Khasanov, H. Luetkens, M. Birke, E. M. Forgan, Ch. Niedermayer, M. Pleines, NIM **B192,** 254 (2002).

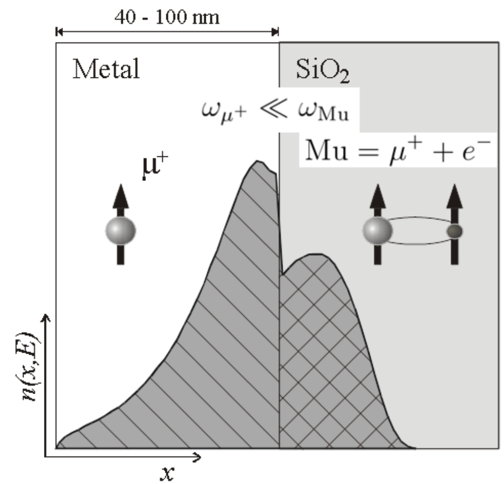

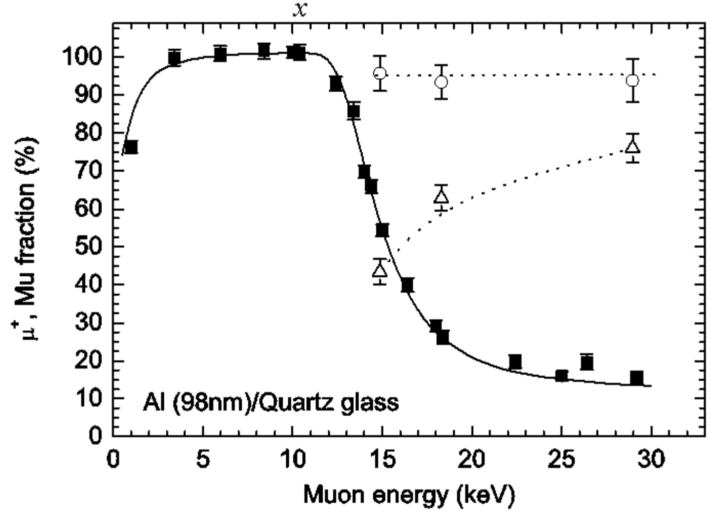

Direct study of 1D field profile by LE-μSR

A superconductor expels a magnetic field from its interior ("Meissner effect")

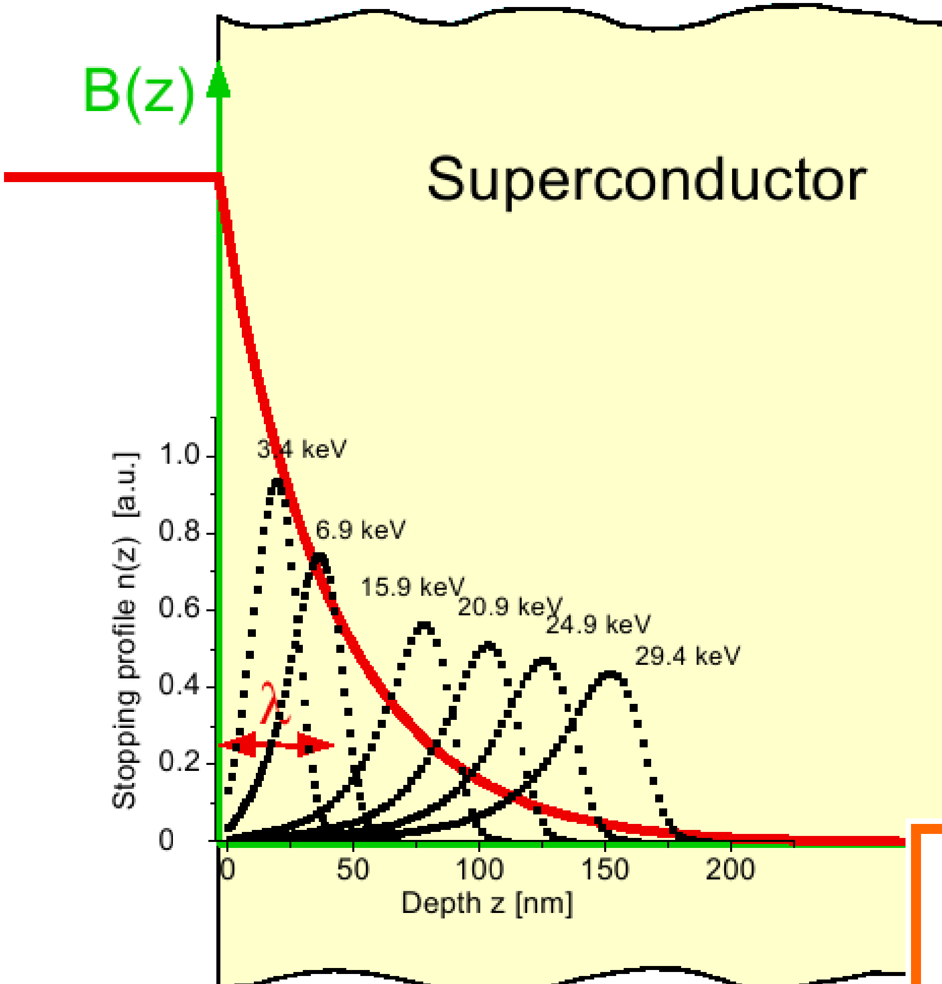

n(z,E): muon implantation profile for a particular muon energy E

μSR experiment ⇒ magnetic field probability distribution p(B, E) sensed by the muons

$$n(z,E)\,\mathrm{d}z = p(B,E)\,\mathrm{d}B$$

$$\int_0^z n(\zeta,E)\,\mathrm{d}\zeta = \int_{B(z)}^{\infty} p(\beta,E)\,\mathrm{d}\beta$$

⇒ B(z)

→ Magnetic field profile B(z) over nm scale

→ Characteristic lengths of the sc λ, ξ

In-plane anisotropy in $YBa_2Cu_3O_{6.92}$

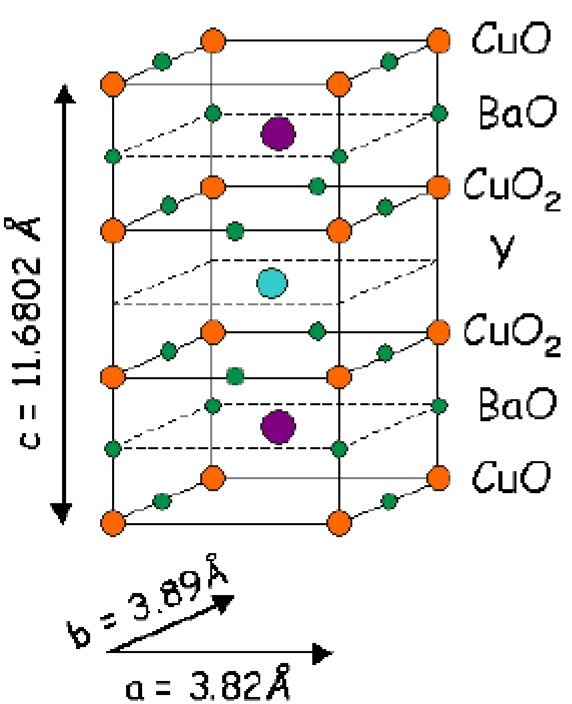

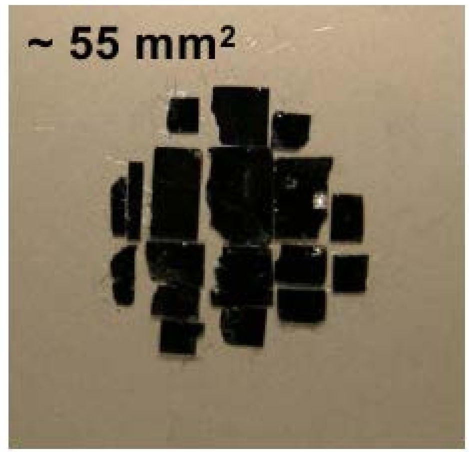

Detwinned (>95%) $YBa_2Cu_3O_{6.95}$ crystals optimally doped
(T_c= 94.1 K, $\Delta T_c \leq$ 0.1K)

samples produced by R. Liang, W. Hardy, D. Bonn, Univ. of British Columbia;

Mosaic of samples glued onto the Ni coated sample plate of the LEM cryostat.

$$\lambda(T) \propto \sqrt{\frac{m^*}{n_s(T)}}$$

←**effective mass**
←**density of super carriers**

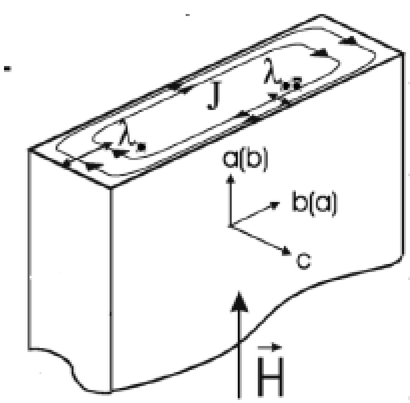

$$\vec{H}_{ext} \parallel \hat{a}\text{-axis} \rightarrow \lambda_b$$

$$\vec{H}_{ext} \parallel \hat{b}\text{-axis} \rightarrow \lambda_a$$

$1/\lambda^2 \sim n_s/m^* \equiv \rho_s$, superfluid density

T-dependence: symmetry of the SC gap

$YBa_2Cu_3O_{6.92}$, T_c = 94 K, B = 9.47 mT

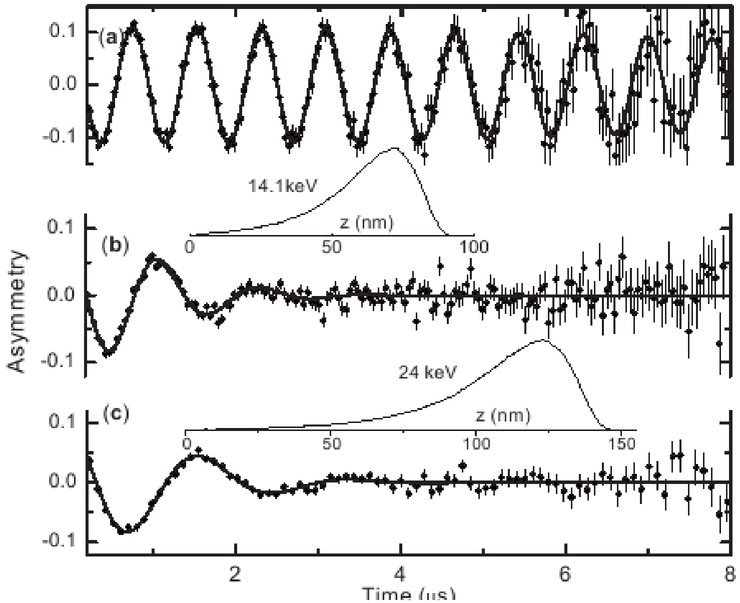

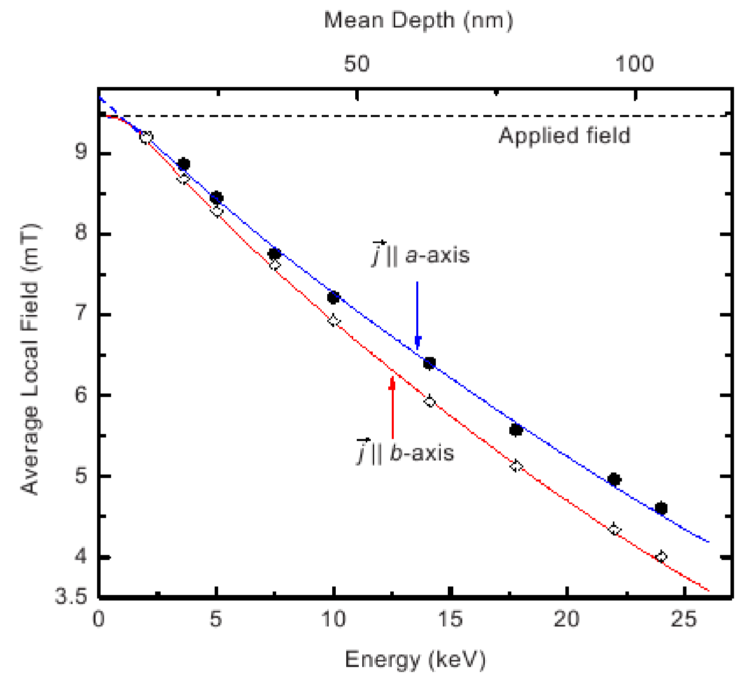

$$B(z) = \begin{cases} B_0 \exp[-(z-d)/\lambda_{a,b}] & z \geq d \\ B_0 & z < d, \end{cases} \qquad (1)$$

$$\mathcal{A}(t) = A \exp[-\sigma^2 t^2/2] \int \rho(z) \cos[\gamma_\mu B(z)t + \phi] dz, \qquad (2)$$

($\rho(z)$: muon stopping profile)

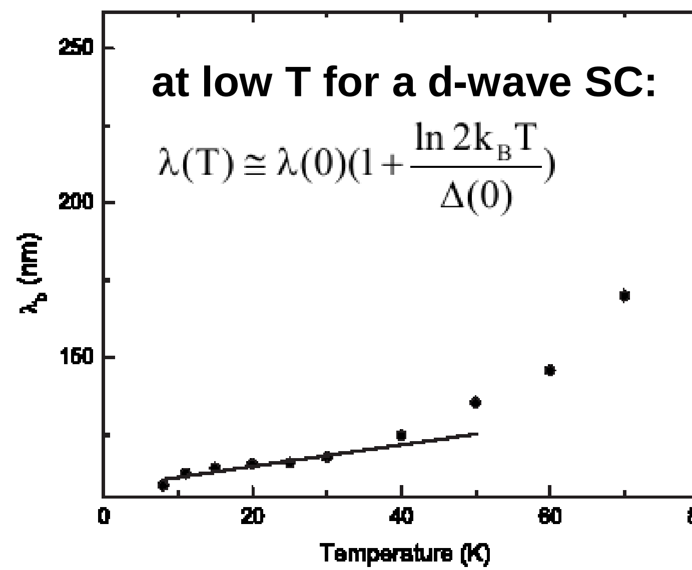

d-wave superconductor

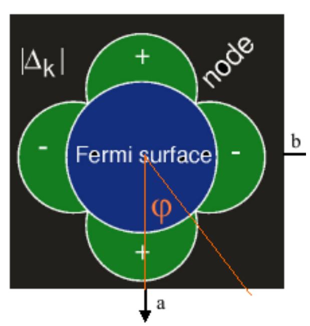

λ_a = 126(1.2)nm, λ_b = 105.5(1.0) nm, λ_a/λ_b = 1.19(1)

R.F. Kiefl et al, Phys. Rev. **B81**, 180502(R), (2010)

1^{st} direct observation of non-local effects in Pb; comparison to $YBa_2Cu_3O_{7-\delta}$

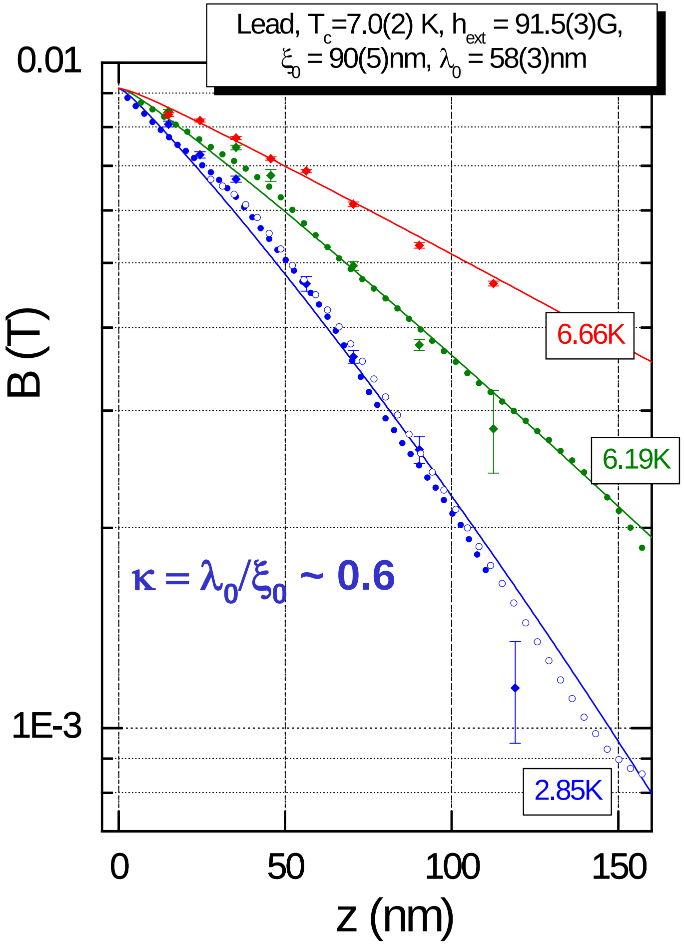

Non-local: non-exponential

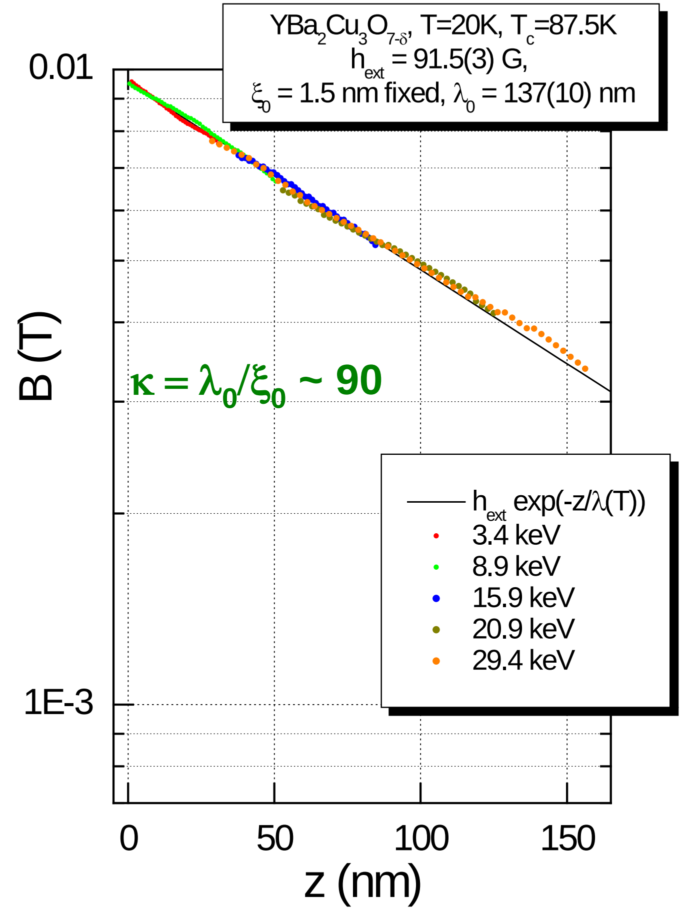

local: exponential

1^{st} experimental determination of ξ_0 in a non-local superconductor; confirmation of some predictions of BCS (~50 years after theory!!)

T.J. Jackson et al., Phys. Rev. Lett. **84**, 4958 (2000).

A. Suter et al., Phys. Rev. Lett. **92**, 087001 (2004).

A. Suter et al., Phys. Rev. **B72**, 024506 (2005).

Example of photo-induced effects

Persistent change of T_c and superfluid density in underdoped $YBa_2Cu_3O_{6+x}$

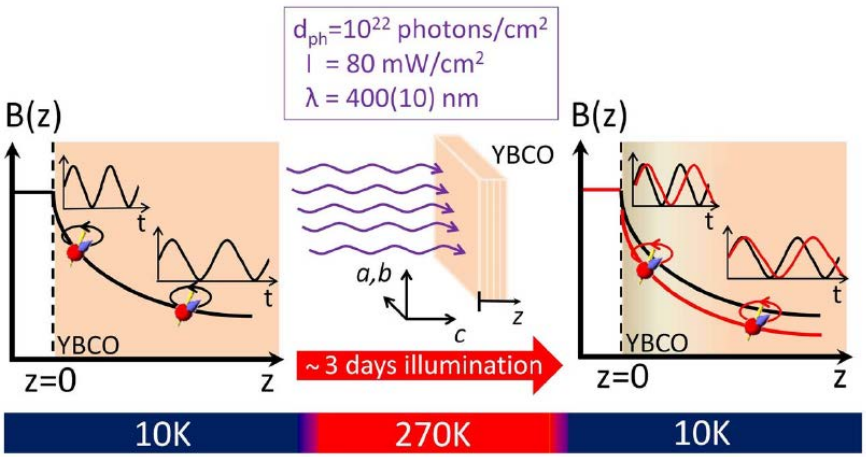

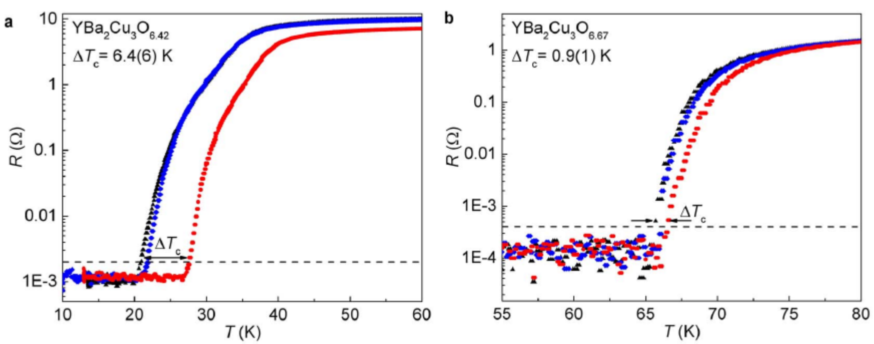

E. Stilp et al, Scientific Reports **4**, 6250 (2014).

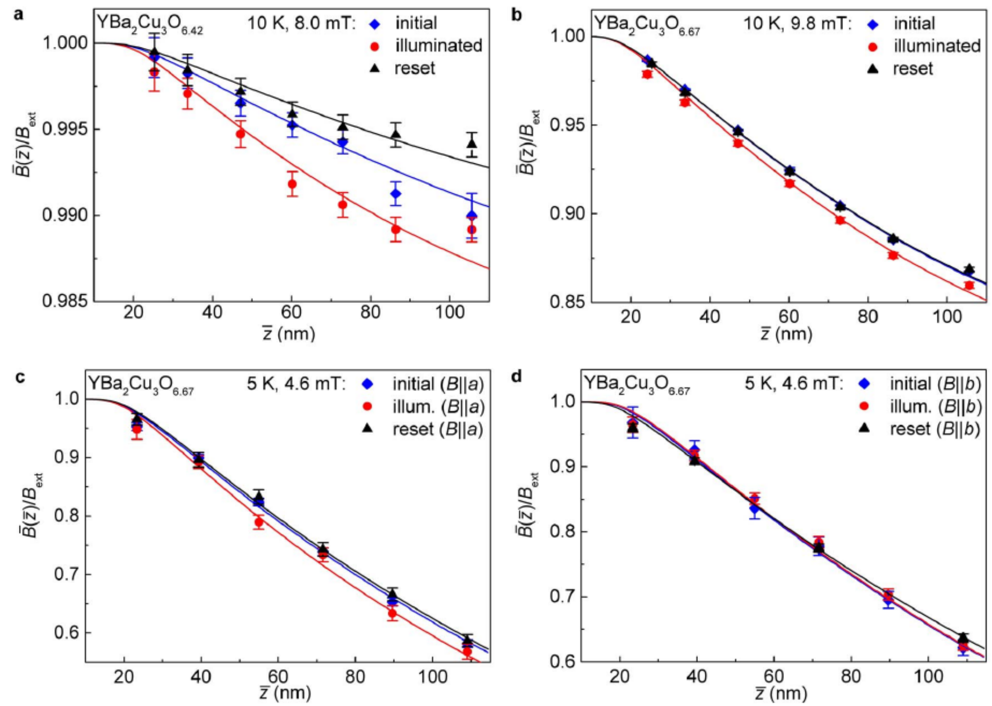

- Studies on photo-persistent conductivity in cuprates have been limited to structural and transport properties

- Here, for the 1st time, using low-energy muons, a strongly increased superfluid density is observed within the first few tens of nanometers after illumination
- attributed to stimulated self-organization of Cu-O chains, reducing nano-scale disorder and thus strengthening the superconducting ground state.

LE-μSR reveals „remote Meissner screening“

Remotely induced magnetism in a normal metal using a superconducting spin valve

M.G. Flokstra et al., Nature Physics **12**, 57 (2016)

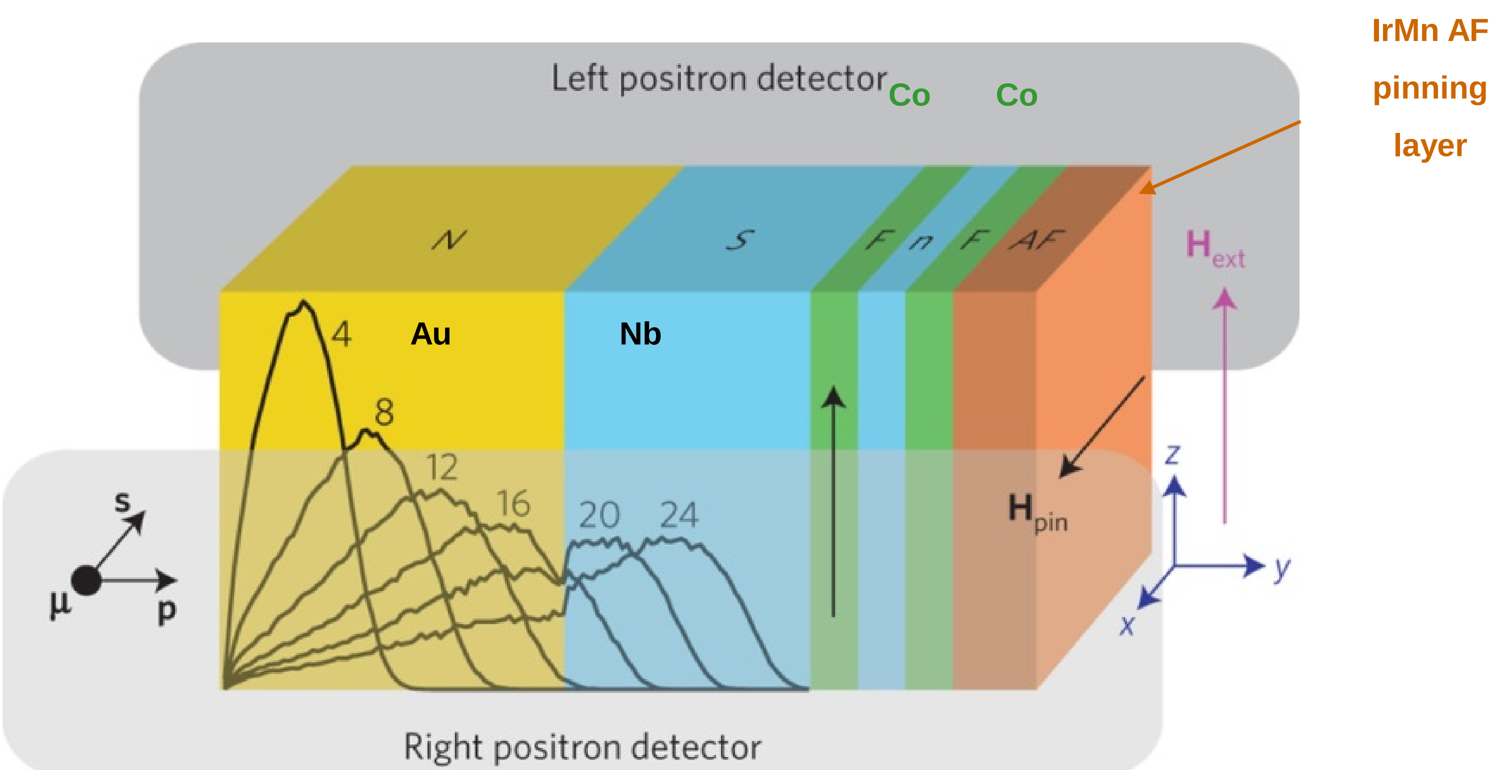

LE-μSR reveals „remote Meissner screening“

M.G. Flokstra et al., Nature Physics **12**, 57 (2016)

- Superconducting spintronics as a promising new field: utilize the internal spin structure of superconducting Cooper pairs
- Basic building blocks: spin-triplet Cooper pairs with equally aligned spins; generated by proximity of a conventional superconductor to a ferromagnetic material
- LE-μSR shows an unanticipated effect in contradiction with existing theoretical models: appearance of magnetization in a remote non-magnetic Au layer separated from the ferromagnetic material
- Control by temperature or by magnetic field: may act as a basic building block for a new generation of quantum interference devices based on the spin of a Cooper pair

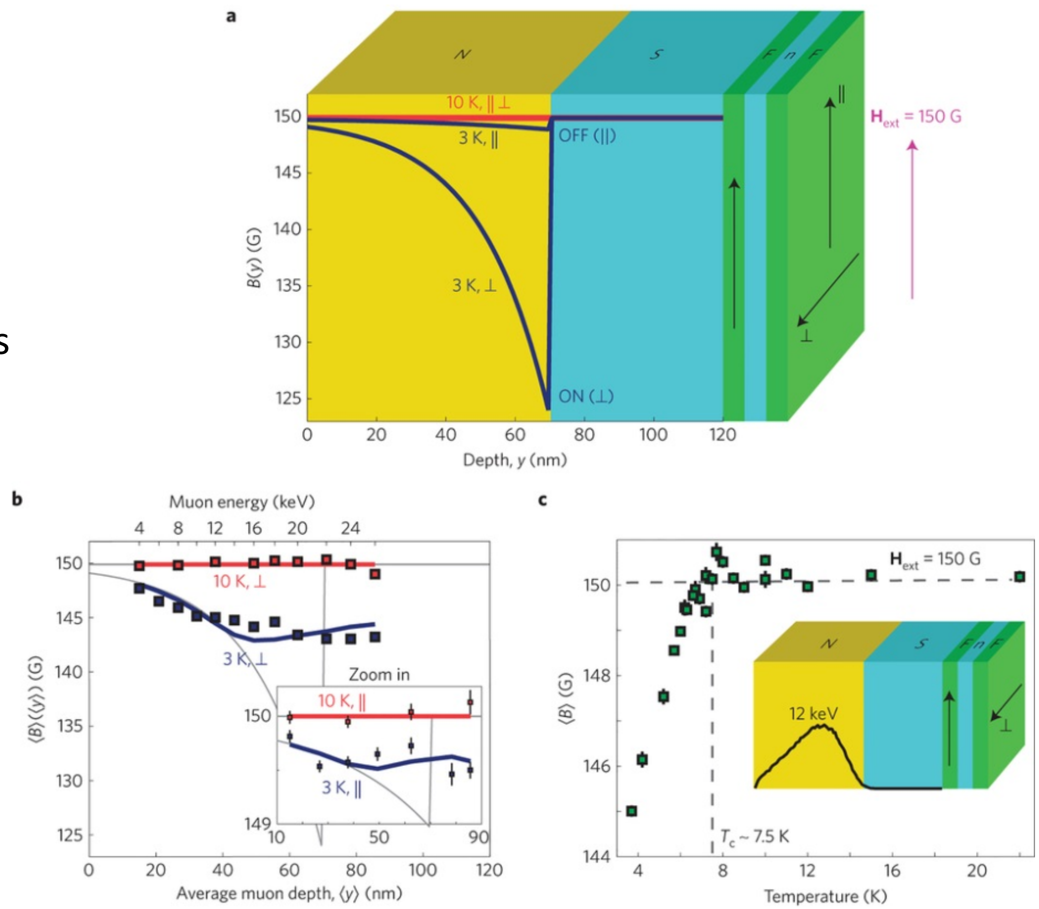

LE-μSR: magnetic order at molecular interfaces

Beating the Stoner Criterion using Molecular Interfaces

F. Al Ma'Mari et al., Nature **524**, 69 (2015)

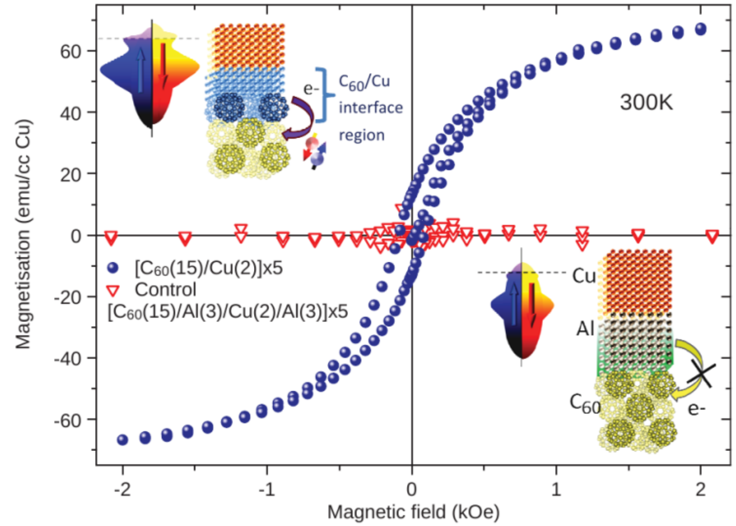

- Unexpected ferromagnetic (FM) ordering at room temperature of non-ferromagnetic thin films (Cu, Mn) and C_{60} molecular layers
- Existence of the emergent FM state over several layers of the metallic films
- Induced magnetism is easily measurable via magnetometry, while LE-μSR indicates localized spin-ordered states close to the metallo-molecular interface
- Density functional theory calculations provide a possible explanation: “magnetic hardening” of the metal atoms due to electron transfer at the interface
- This opens the path to design magnetic metamaterials using abundant, non-toxic elements including organic semiconductors
- Use charge transfer at molecular interfaces to control spin polarization or magnetization (allows the design of new electronic devices)

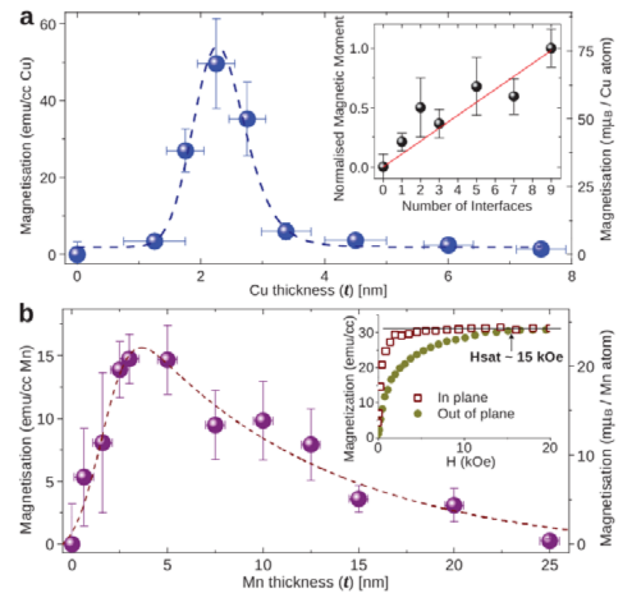

PAUL SCHERRER INSTITUT PSI

LE-μSR: magnetic order at molecular interfaces

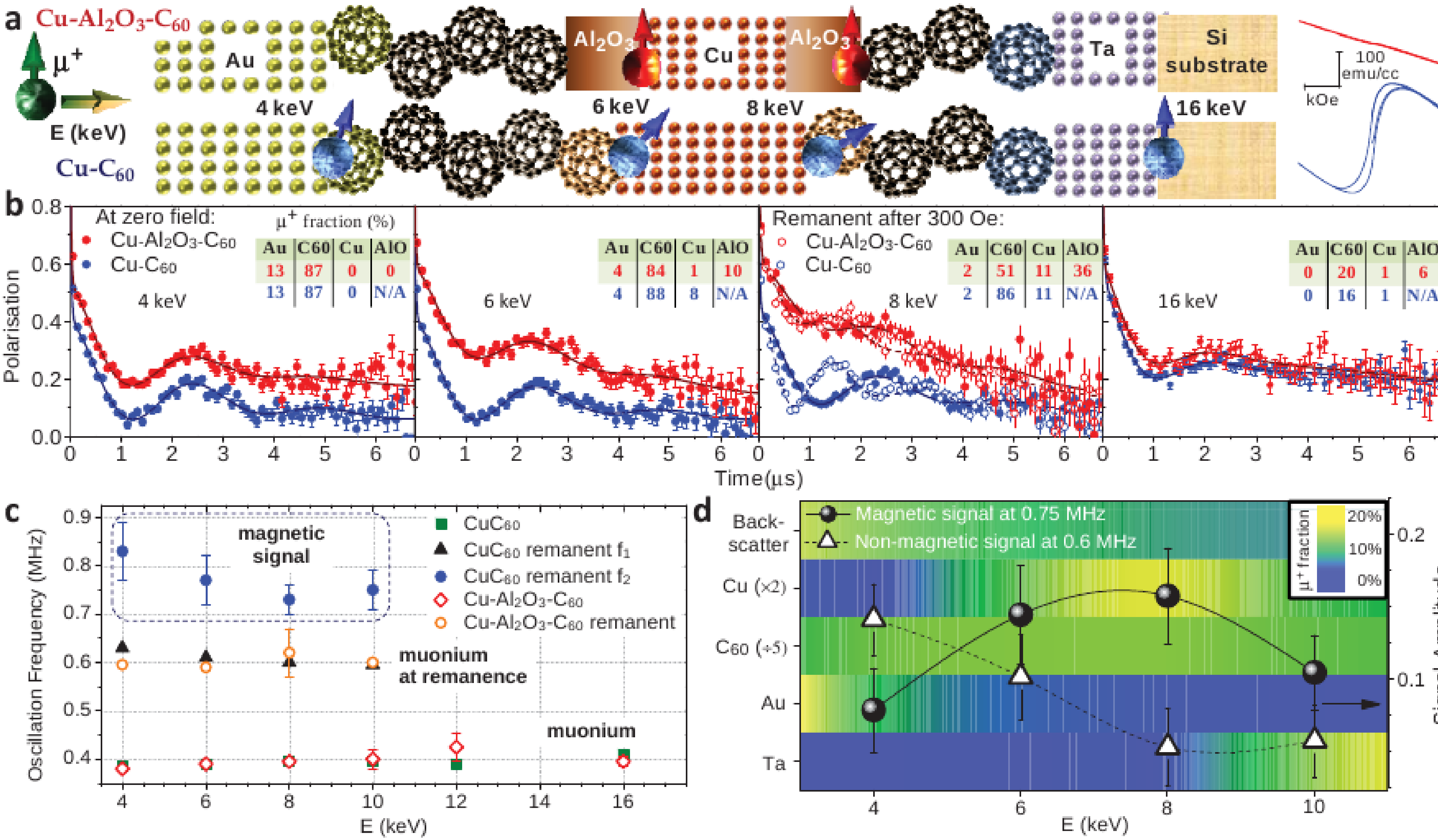

F. Al Ma'Mamari et al., Nature **524**, 69 (2015)

Use of μ^+ to measure charge carrier profiles

- **Controlled manipulation of charge carrier concentration in nanometer-thin layers is the basis of current semiconductor technology**
- Usually, macroscopic transport measurements and modeling are used to determine charge carrier profiles across interfaces
- Low-energy μ^+SR (1-30 keV, mean depths 5-200nm) as a local probe technique can provide hitherto unaccessible direct information about carrier profiles and dynamics at semiconductor surfaces and interfaces (e.g. pn-junctions)
- Use Ge as a prototype system: well studied by bulk μSR; test the feasibility of detecting the variation of charge carriers concentrations at interfaces
- Final goal: application to technologically and scientifically relevant devices: solar cell structures, oxide-semiconductor interfaces, quantum well structures etc.

μ^+SR in semiconductors

- In semiconductors: μ^+ can capture an electron to form the hydrogen pseudo-isotope muonium [Mu^0 (μ^+e^-), mass m_{Mu} ~1/9 m_H]

- Hyperfine-coupling in Mu^0 causes μ^+ precession frequencies to be different to the μ^+ Larmor frequency; Mu^- precession at μ^+ Larmor frequency

- In the presence of free charge carriers cyclic charge exchange reactions may occur:

$$\mu^+ + e^- \leftrightarrow Mu^0 \quad \text{or} \quad Mu^- + h^+ \leftrightarrow Mu^0$$

„fluctuating magnetic field“ at the μ^+ causing depolarization of the μ^+ ensemble;

depolarization rate $\propto$ free charge carrier concentration

Thermally activated ionization of Mu^0 to $Mu^{+/-}$ at a rate Λ_i may be followed by charge capture at a rate Λ_c:

$$\Lambda_i = \Lambda_0 \times exp(-E_A/k_B T)$$

$$\Lambda_c^{e,h} = n \times v_{e,h} \times \sigma_c^{e,h}$$

Mu_T^0 at the tetrahedral interstitial in Ge

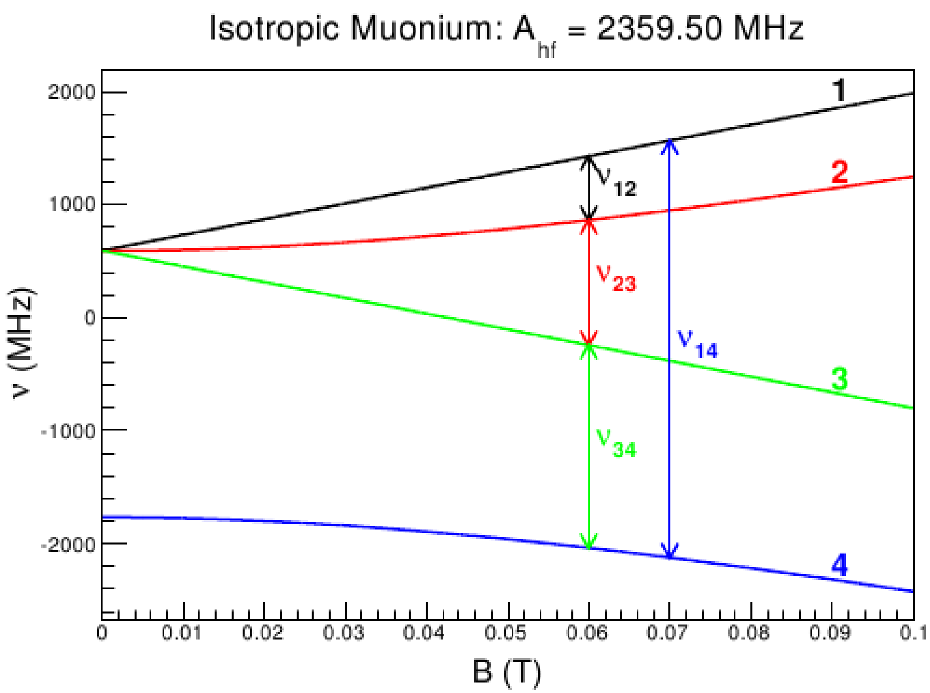

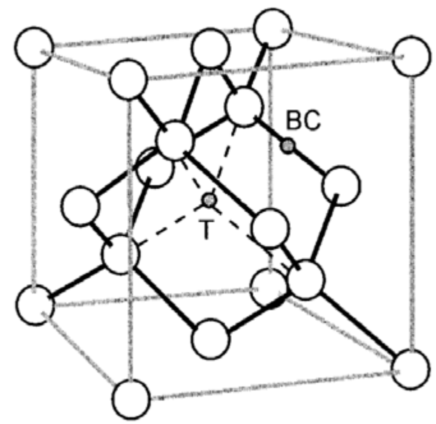

Figure 1. Breit-Rabi diagram with possible transitions ν_{ij} in a transverse magnetic field B of isotropic muonium Mu_T^0 in Ge with a hyperfine coupling of 2359.5 MHz.

Table 1. Transition frequencies and probabilities of isotropic Mu_T^0 in germanium in an applied transverse field of 0.1 T.

transition	frequency (MHz)	probability
ν_{12}	736.9	0.441
ν_{34}	−1622.6	0.441
ν_{23}	2048.8	0.059
ν_{14}	4408.3	0.059

T. Prokscha, J. Phys.: Conf. Ser. ***551****, 012049 (2014)*

μ^+ Larmor frequency = 13.6 MHz at 0.1 T

Simulation: effect of charge-exchange cycles on TF-μSR depolarization rate λ in Ge

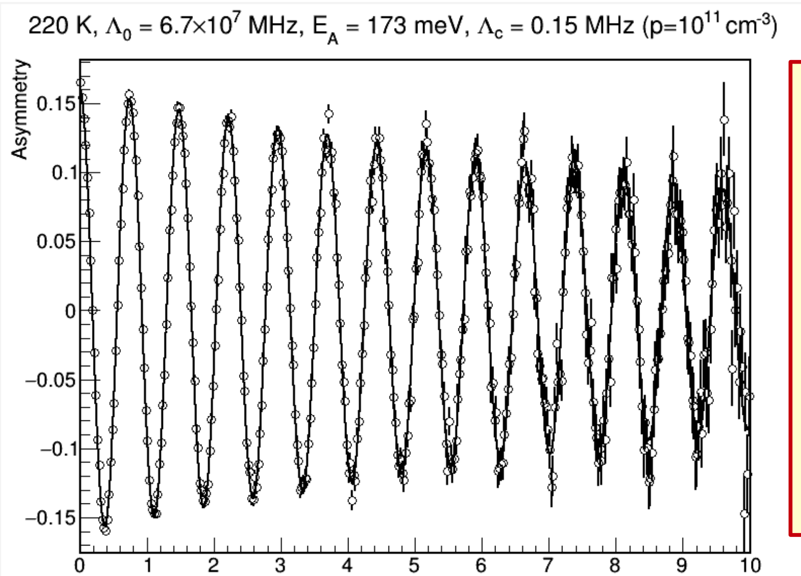

Cyclic charge state transitions: $Mu_T^- + h^+ \rightleftharpoons Mu_T^0$

forward reaction (hole capture):

λ_f: fast transverse-field (TF) μSR relaxation rate,

$\Lambda_c^h = p\, v^h\, \sigma_c^h$ Λ_c^h: hole capture rate

reverse reaction (Mu^0 ionization):

$\Lambda_i = \Lambda_0 \exp(-E_A/k_BT)$ Λ_i: ionization rate, Λ_0=6.7▪10^{13}/s,

E_A ~ 173 meV

[*Lichti et al., PRB **60** (1999)*]

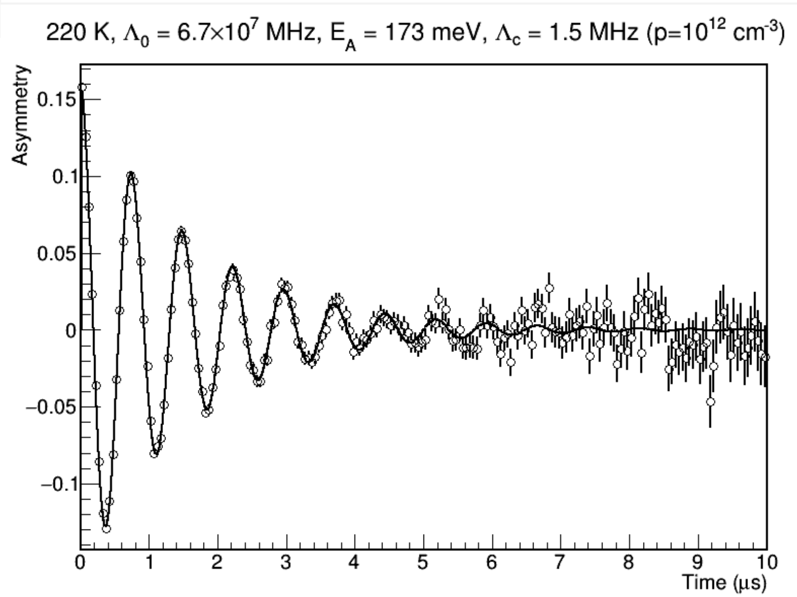

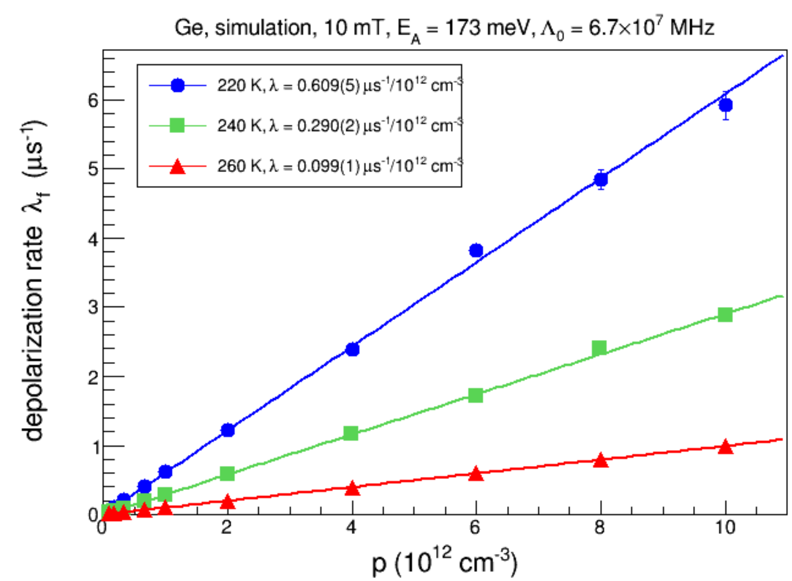

Detection of hole-depleted surface layer in p-Ge

Decay asymmetry A_D of Mu^+/Mu^-

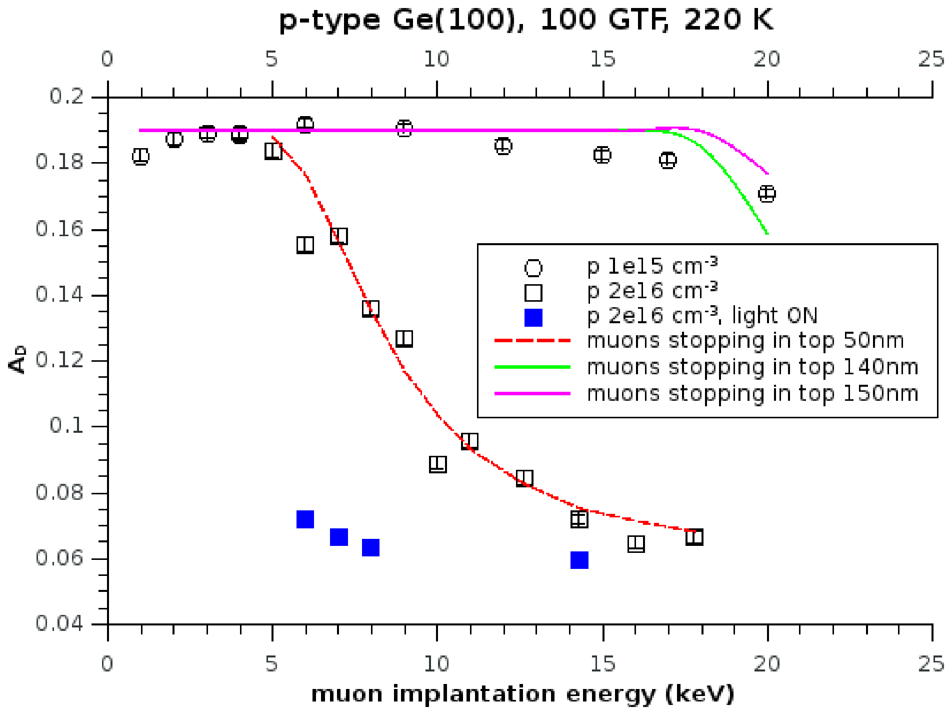

Data imply following p profile:

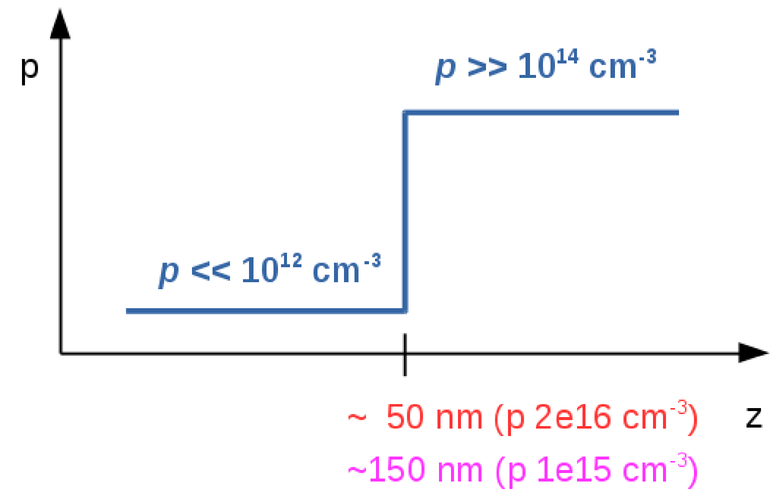

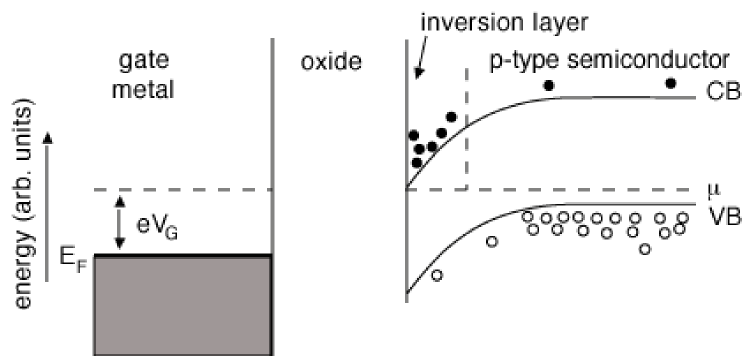

PAUL SCHERRER INSTITUT

p-Ge, 10^{15} cm^{-3}, manipulation of hole depletion layer by red light (635 nm) illumination

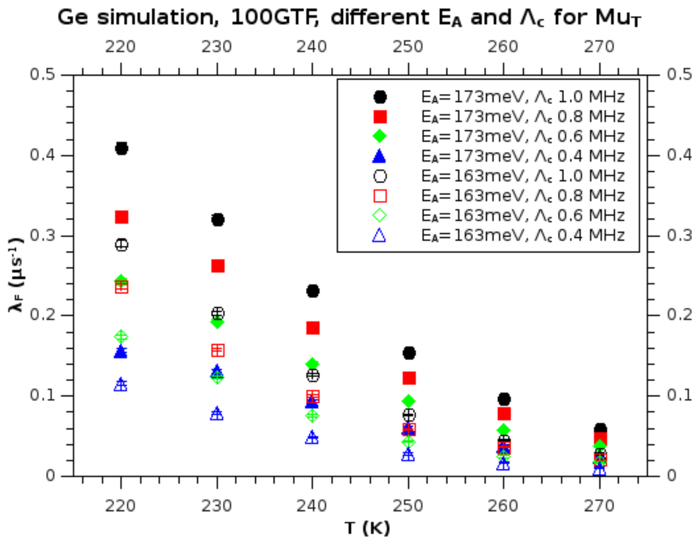

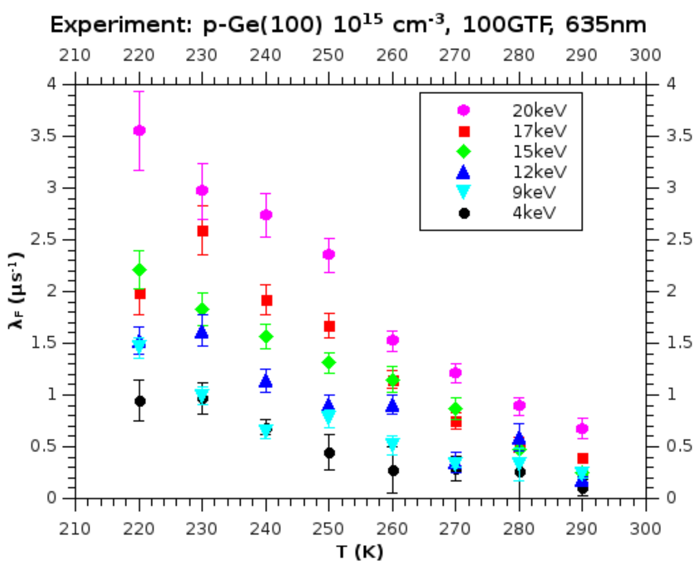

Fit $\lambda_F(T)$ to determine E_A, Λ_c as a function of depth:

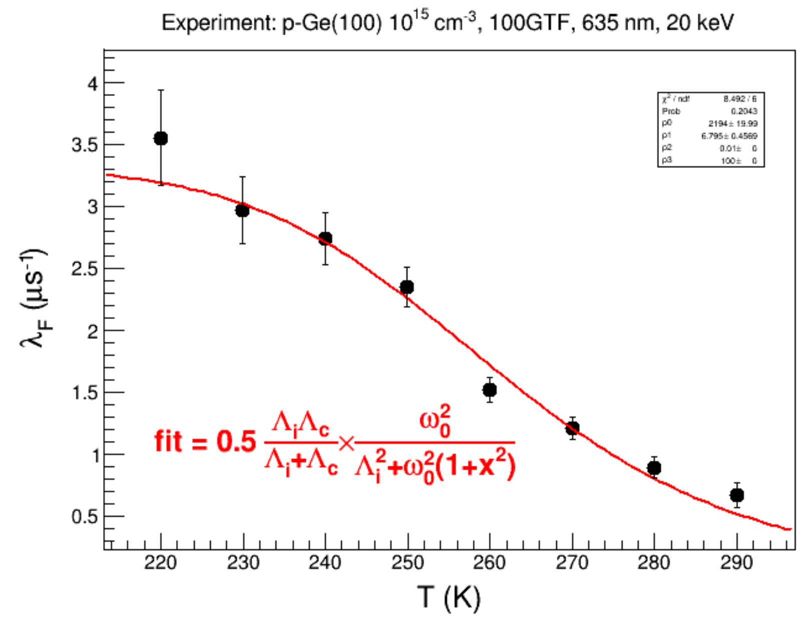

$\Lambda_i = \Lambda_0 \exp(-E_A/k_BT)$: Mu_T^0 ionization rate

$\Lambda_c = p\, v^h\, \sigma_c^h$: Mu_T^- hole capture rate

ω_0: Mu_T^0 hyperfine coupling

$x = B/B_0$, with B_0 = 842 G the “hyperfine field”

p-Ge, 10^{15} cm^{-3}, manipulation of hole depletion layer by red light (635 nm) illumination

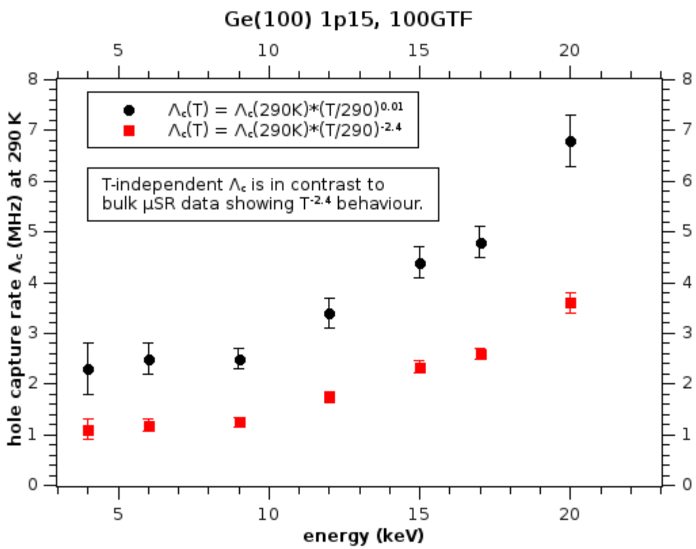

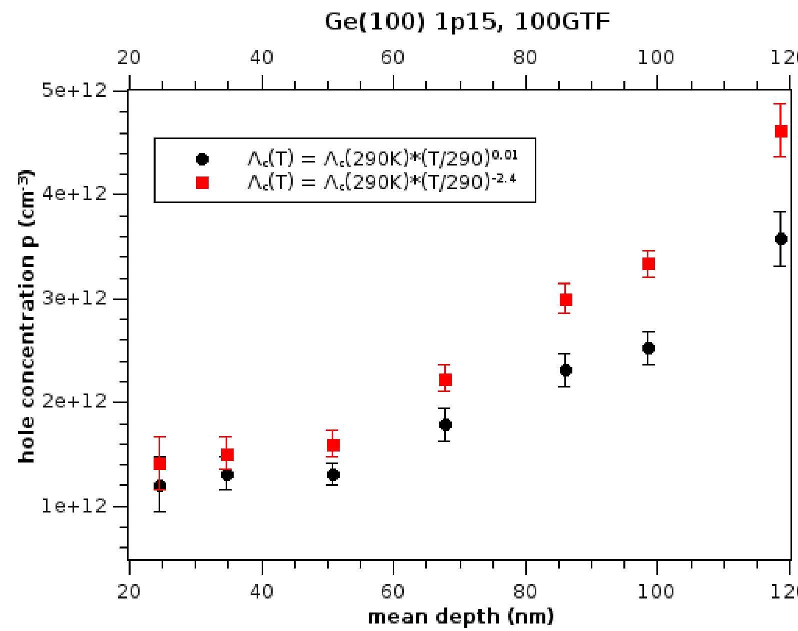

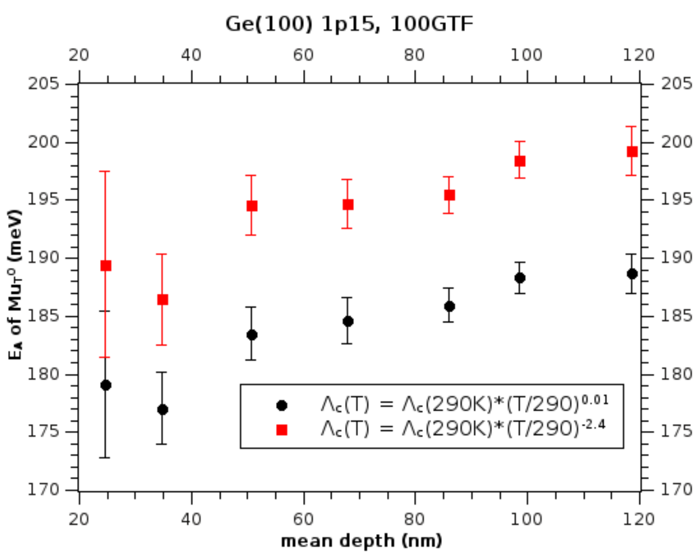

- 1st observation of a carrier concentration gradient at the surface of a depleted semiconductor by a local probe technique

- Indication of an increasing Mu_T^0 activation energy as a function of depth: band bending/electric fields at the surface

(T. Prokscha et al. PRB 90, 235303 (2014))

More LE-μSR applications

Surface dynamics of polymers

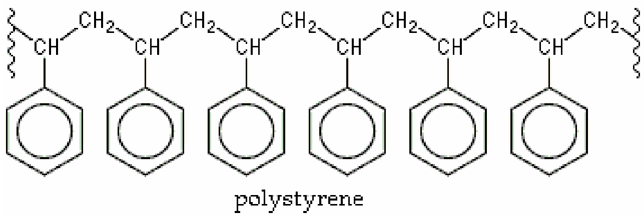

F.L. Pratt et al., *PRB* ***72****, 121401(R) (2005)*
F.L. Pratt et al., *Polymer* ***105****, 516 (2016)*

Magnetic properties of monolayers of single molecule magnets

Z. Salman et al.

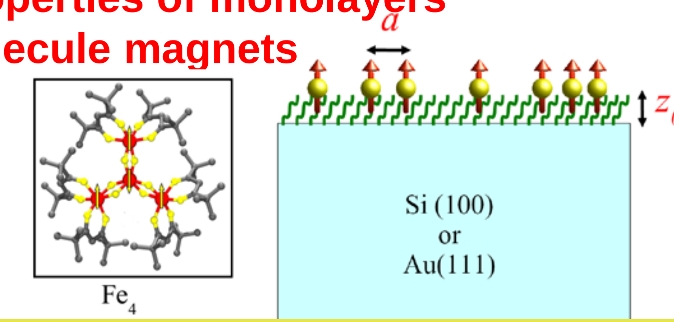

http://www.psi.ch/low-energy-muons/lem-publications

Formation of hydrogen impurities in semiconductors at low energies

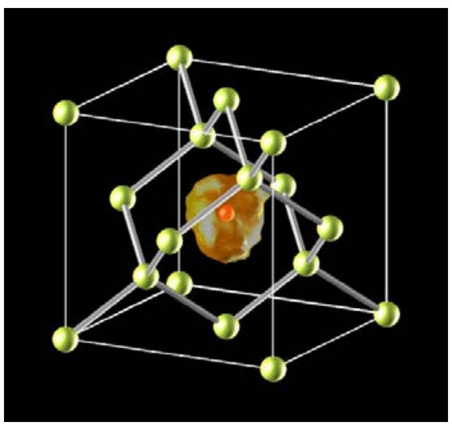

T. Prokscha et al., *PRL* ***98****, 227401 (2007)*
T. Prokscha et al., *Physcia* ***B 404****, 866 (2009)*
D.G. Eshchenko et al., *Physica* ***B 404****, 873 (2009)*
H.V. Alberto et al., *Physica* ***B 404****, 870 (2009)*

Photo-induced effects in semiconductors

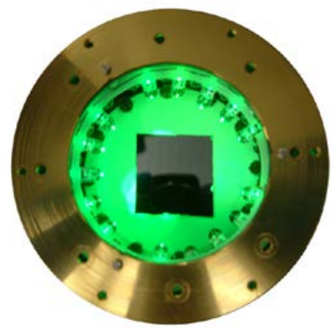

T. Prokscha et al., Sci. Rep. ***3,*** *2569 (2013)*

Superconductivity and Magnetism in $La_2CuO_4/La_{1.56}Sr_{0.44}CuO_4$ Superlattices

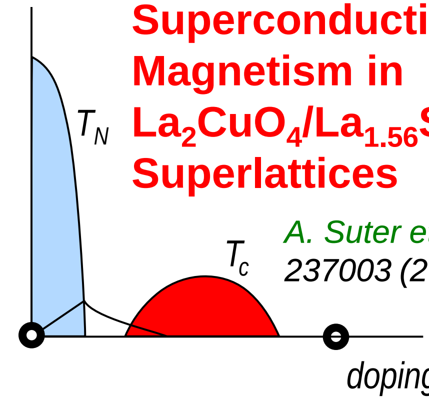

A. Suter et al., *PRL* ***106****, 237003 (2011)*

Current effects on magnetism and superconductivity in a thin $La_{1.94}Sr_{0.06}CuO_4$ wire

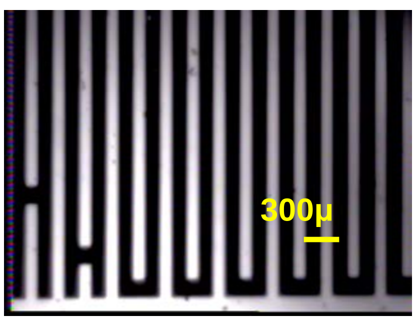

M. Shay et al., *PRB* ***80****, 144511 (2009)*

Superfluid density in high and low T_c heterostructures

B. Wojek et al., *PRB* ***85****, 024505 (2012)*

Superconductivity and magnetism in electron doped cuprates

H. Saadaoui et al., Nat. Comm. ***6****, 6041 (2015)*

Laboratory for Muon Spin Spectroscopy

Alex Amato (LMU Head)
Isolde Fuchs (Secretary)
Elvezio Morenzoni
Andrea-Raeto Raselli (Computing)

Bulk µSR
Hubertus Luetkens (GPS)
Christopher Baines (LTF)
Robert Scheuermann (HAL-9500)
Rustem Khasanov (GPD)
Jean-Christophe Orain (PostDoc, Dolly)
Joel Barker (PostDoc)
Gediminas Simutis (PostDoc)
Artem Nikitin (PostDoc, COFUND)
Stefan Holenstein (PhD, Uni ZH)
Matthias Elender (Techn.)

Low Energy µSR
Thomas Prokscha (LEM)
Andreas Suter (LEM)
Zaher Salman (LEM)
Jonas Krieger (PhD, ETHZ)
Hans-Peter Weber (Techn.)

Thank you for your attention!